Geological Society, London, Special Publications

Oligocene–Miocene basin evolution in SE Anatolia, Turkey: constraints on the closure of the eastern Tethys gateway

Silja K. Hüsing, Willem-Jan Zachariasse, Douwe J. J. van Hinsbergen, Wout Krijgsman, Murat Inceöz, Mathias Harzhauser, Oleg Mandic and Andreas Kroh

Geological Society, London, Special Publications 2009, v.311; p107-132.
doi: 10.1144/SP311.4

Notes

Oligocene–Miocene basin evolution in SE Anatolia, Turkey: constraints on the closure of the eastern Tethys gateway

SILJA K. HÜSING[1]*, WILLEM-JAN ZACHARIASSE[2], DOUWE J. J. VAN HINSBERGEN[1], WOUT KRIJGSMAN[1], MURAT INCEÖZ[3], MATHIAS HARZHAUSER[4], OLEG MANDIC[4] & ANDREAS KROH[4]

[1]*Paleomagnetic Laboratory "Fort Hoofddijk", Department of Earth Sciences, Utrecht University, Budapestlaan 4, 3584 CD Utrecht, The Netherlands*

[2]*Stratigraphy and Paleontology Group, Department of Earth Sciences, Utrecht University, The Netherlands*

[3]*Department of Geology, Fırat University, Elazığ, Turkey*

[4]*Natural History Museum Vienna, Austria*

**Corresponding author (e-mail: huesing@geo.uu.nl)*

Abstract: The Oligocene–Miocene was a time characterized by major climate changes as well as changing plate configurations. The Middle Miocene Climate Transition (17 to 11 Ma) may even have been triggered by a plate tectonic event: the closure of the eastern Tethys gateway, the marine connection between the Mediterranean and Indian Ocean. To address this idea, we focus on the evolution of Oligocene and Miocene foreland basins in the southernmost part of Turkey, the most likely candidates to have formed this gateway. In addition, we take the geodynamic evolution of the Arabian–Eurasian collision into account.

The Muş and Elazığ basins, located to the north of the Bitlis–Zagros suture zone, were most likely connected during the Oligocene. The deepening of both basins is biostratigraphically dated by us to occur during the Rupelian (Early Oligocene). Deep marine conditions (between 350 and 750 m) prevailed until the Chattian (Late Oligocene), when the basins shoaled rapidly to subtidal/intertidal environment in tropical to subtropical conditions, as indicated by the macrofossil assemblages. We conclude that the emergence of this basin during the Chattian severely restricted the marine connection between an eastern (Indian Ocean) and western (Mediterranean) marine domain. If a connection persisted it was likely located south of the Bitlis–Zagros suture zone. The Kahramanmaraş basin, located on the northern Arabian promontory south of the Bitlis–Zagros suture zone, was a foreland basin during the Middle and Late Miocene, possibly linked to the Hatay basin to the west and the Lice basin to the east. Our data indicates that this foreland basin experienced shallow marine conditions during the Langhian, followed by a rapid deepening during Langhian/Serravallian and prevailing deep marine conditions (between 350 and 750 m) until the early Tortonian. We have dated the youngest sediments underneath a subduction-related thrust at *c.* 11 Ma and suggest that this corresponds to the end of underthrusting in the Kahramanmaraş region, i.e. the end of subduction of Arabia. This age coincides in time with the onset of eastern Anatolian volcanism, uplift of the East Anatolian Accretionary Complex, and the onset of the North and East Anatolian Fault Zones accommodating westward escape tectonics of Anatolia. After *c.* 11 Ma, the foreland basin south of the Bitlis formed not (or no longer) a deep marine connection along the northern margin of Arabia between the Mediterranean Sea and the Indian Ocean. We finally conclude that a causal link between gateway closure and global climate change to a cooler mode, recorded in the Mi3b event ($\delta^{18}O$ increase) dated at 13.82 Ma, cannot be supported.

Tectonic closure and opening of marine gateways is suggested to have led to substantial reorganization of surface and deep ocean water currents and may have caused important changes in global climate. The closure of the Panama Isthmus between 3.0 and 2.5 Ma has influenced the Gulf Stream, triggering major Northern Hemisphere glaciations (Bartoli *et al.* 2005; Schneider & Schmittner 2006). The opening of the Drake Passage allowed the start of the Antarctic Circumpolar Current which might have initiated the abrupt climate cooling around the Eocene/Oligocene boundary and the extensive growth of Antarctic ice sheets (Livermore *et al.* 2005). The restriction of water exchange across

From: van Hinsbergen, D. J. J., Edwards, M. A. & Govers, R. (eds) *Collision and Collapse at the Africa–Arabia–Eurasia Subduction Zone*. The Geological Society, London, Special Publications, **311**, 107–132.
DOI: 10.1144/SP311.4 0305-8719/09/$15.00

the former straits between Spain and Morocco resulted in the desiccation of the Mediterranean Sea during its Messinian Salinity Crisis (Hsü *et al.* 1973). Likewise, the disconnection of the Indian Ocean and the Atlantic/Mediterranean water masses has been suggested to have caused a major middle Miocene climate change, widely recognized in both the marine (Woodruff & Savin 1989; Flower & Kennett 1994; Zachos *et al.* 2001; Bicchi *et al.* 2003) and the terrestrial record (Krijgsman *et al.* 1994). It is this disconnection that forms the scope of this paper.

The middle Miocene is a period characterized by major environmental changes during which the Earth's climate gradually progressed into a colder mode (Zachos *et al.* 2001). The Miocene Climate Optimum between 17 to 15 Ma was followed by an interval of global climate variability between 15 and 14 Ma, marked by atmospheric and oceanic cooling, East Antarctic Ice Sheet growth, and carbon cycle variability (Woodruff & Savin 1989; Flower & Kennett 1994; Zachos *et al.* 2001). Seven major δ^{18}O shifts, Mi1 to Mi7, to higher (= colder) values documented in marine records of the Atlantic reflect brief periods of increased glaciations (Miller *et al.* 1991; Wright *et al.* 1992; Miller *et al.* 2005). The Mi3a, Mi3b and Mi4 events between about 14.5 and 12.5 Ma represent the middle Miocene δ^{18}O increase, leading the global climate into a colder mode at the same time as the onset of the Antarctic glaciations (van der Zwaan & Gudjonsson 1986; Abels *et al.* 2005; Miller *et al.* 2005).

A direct relationship between the Middle Miocene Climate change, whether recorded in oxygen or carbon isotopes, marine or terrestrial fauna, and the closure of the eastern Tethys gateway has so far never been proven, although many studies suggest a causal link between the two events (e.g. Woodruff & Savin 1989; Rögl 1999; Flower & Kennett 1993). Part of the problem is that the sediments that were deposited in the eastern Tethys gateway have on many occasions not been recognized or properly dated. In addition, the chronological sequence of tectonic processes involved in the convergence of the Eurasia and African–Arabian plates is complex and actively debated (see Garfunkel 1998, 2004; Golonka 2004). To assess the timing of gateway closure along the northern Arabian promontory, the major geodynamic processes of the Arabia–Eurasia collision and their tectonic responses have to be taken into account. According to reconstructions of Jolivet & Faccenna (2000) and Bellahsen *et al.* (2003), Arabia collided first in the eastern Anatolian/western Iranian region around 30 Ma ago. Consequently, it gradually rotated counterclockwise leading to diachronous collision eastward from Southeastern Anatolia towards the Persian Gulf (Hessami *et al.* 2001). Therefore, we decided to study the southernmost flysch deposits in eastern Anatolia (Fig. 1), these being the most likely candidates to represent the youngest sediments deposited just prior to the disconnection of the Indian–Arabian gateway.

Geodynamic and geological context

The continental collision of the African–Arabian plate with the Eurasian plate resulted in a tectonic collage in eastern Anatolia that is generally subdivided into: (1) the eastern Rhodope–Pontide Arc in the north; (2) the East Anatolian Accretionary Complex consisting of an ophiolitic mélange overlain by Paleocene to upper Oligocene sediments; and (3) the Bitlis–Pötürge Massif tectonically overlying the northern part of the Arabian margin (Fig. 1) (Şengör & Yılmaz 1981; Yılmaz 1993; Tüysüz & Erler 1995; Robertson 2000; Şengör *et al.* 2003; Agard *et al.* 2005). As north–south shortening continued between the converging Eurasian and Arabian plate, the relatively soft and irresistant East Anatolian Accretionary Complex took up most of the initial post-collisional convergent strain by shortening and thickening (Yılmaz *et al.* 1998). Around 13–11 Ma, eastern Anatolia underwent rapid uplift and was confronted with onset of widespread volcanism (Dewey *et al.* 1986; Pearce *et al.* 1990; Keskin 2003; Şengör *et al.* 2003), which has been associated with detachment of northward dipping subducted lithosphere (Keskin 2003; Faccenna *et al.* 2006; Hafkenscheid *et al.* 2006). From this moment onward, the ongoing northward motion of Arabia (still continuing today) (McClusky *et al.* 2000; Reilinger *et al.* 2006; Allmendinger *et al.* 2007), and the retreat of the Hellenic subduction zone to the west (Berckhemer 1977; Le Pichon *et al.* 1982; Jolivet 2001) led to westward tectonic escape of Anatolia along the North and East Anatolian Faults (Dewey & Şengör 1979; Şengör *et al.* 1985).

The present-day plate boundary of the African and Eurasian plates is determined by the Bitlis–Zagros suture zone (Robertson 2000 and references therein; Westaway 2003). On the Arabian plate, to the south of the suture zone, Eocene and younger (volcano-) sediments are relatively flat lying. North of the Bitlis–Pötürge zone, Tertiary marine sediments crop out rarely and the geology is dominated by pre-Neogene basement rocks (metamorphic rocks) and Neogene volcanic rocks. The Bitlis–Pötürge Massif itself is characterized by a stack of nappes originated on the Eurasian side of the Neotethys (Robertson 2000; Robertson *et al.* 2004).

The Bitlis–Pötürge Massif runs from southeastern Turkey to the eastern Mediterranean basin into the Cyprus arc, where it meets the East Anatolian

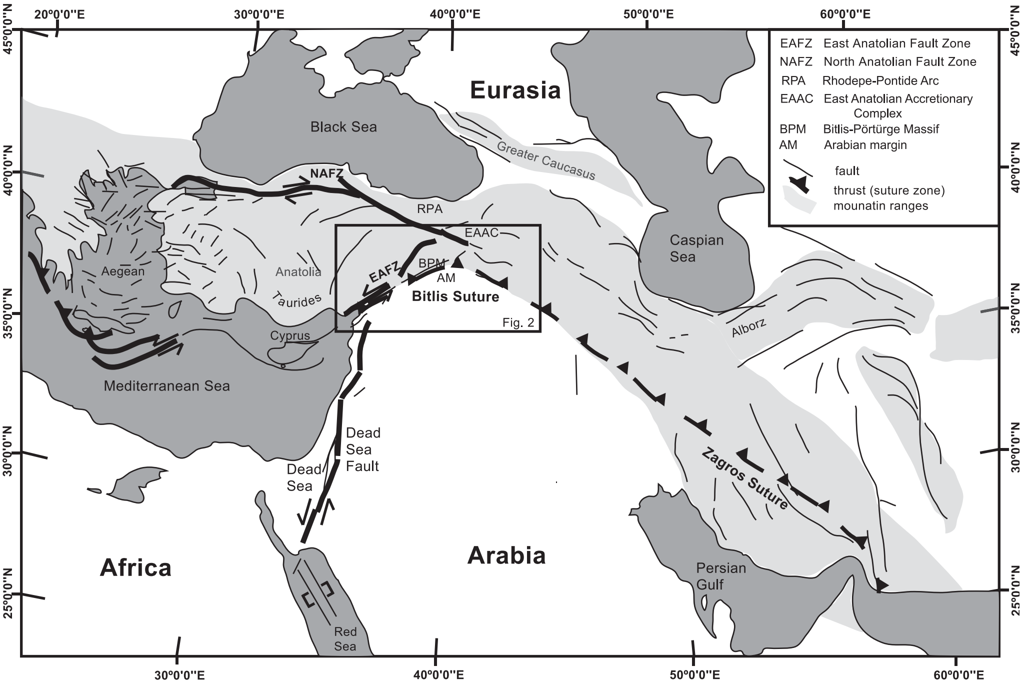

Fig. 1. Outline of tectonic map of the Middle East region, showing major structures such as the Bitlis–Zagros Suture zone, the North and East Anatolian Fault Zones (NAFZ and EAFZ), and mountain ranges related to the convergence of Africa–Arabia and Eurasia (drawn after Geological map of Turkey (Şenel 2002)).

Fault (EAF). Here the structure becomes more complex with several sub-parallel southwestwards running faults and thrusts. The East Anatolian Fault is a 2–3 km wide, active left-lateral strike-slip fault extending from Antakya in the west to Karliova in the NE, where it meets the eastern termination of the North Anatolian Fault (NAF) (Figs 1 & 2; EAFZ and NAFZ). The NAF is a right-lateral strike-slip fault extending over a length of about 1300 km westward. The relative Africa–Arabia motion is taken up by strike-slip displacement along the Dead Sea Fault (Jolivet & Faccenna 2000), while the Africa–Anatolia motion is taken up by subduction south of Cyprus. The overall convergence between Arabia and Anatolia is taken up along the North and East Anatolian fault zones (NAFZ and EAFZ) (Fig. 2) (e.g. McClusky *et al.* 2000; Şengör *et al.* 2005). There is general consensus that the NAFZ and EAFZ had the majority of their displacement in Plio-Pleistocene times (Barka 1992; Westaway 2003, 2004; Hubert-Ferrari *et al.* 2008) although incipient motion may have been as early as late Serravallian/early Tortonian (*c.* 12 to 11 Ma) (Dewey *et al.* 1986; Hubert-Ferrari *et al.* 2002, 2008; Bozkurt 2003; Şengör *et al.* 2005).

The region that comprises the eastern Tethys gateway has thus been subjected to plate convergence and subduction. Şengör *et al.* (2003) suggested that this subduction led to southward migrating accretion of nappes and overlying deep-marine foreland basin deposits, even though individual basins that may reflect such evolution have not been identified in the geological record, which is, at least in part, due to the young volcanic sequences covering a large part of eastern Turkey. If southward accretion of nappes indeed occurred, one should be able to identify southward younging flysch deposits (e.g. van Hinsbergen *et al.* 2005*a*). A foredeep likely remains present until continent–continent collision and subsequent slab break-off stalls convergence and the collision zone is uplifted. Even though small marine basins may remain, the long distance between the Persian Gulf and the Mediterranean Sea makes foredeeps the most promising basins to have formed the gateway between these water masses. In the following paragraphs we will present and discuss the evolution of foredeep basins in SE Turkey in the light of the closure of the eastern Tethys gateway.

Basin evolution

The Arabian foreland is separated from the East Anatolian Accretionary Complex (EAAC) by the Bitlis–Pötürge Massif (Fig. 1). The area of this massif corresponds to the compression zone located

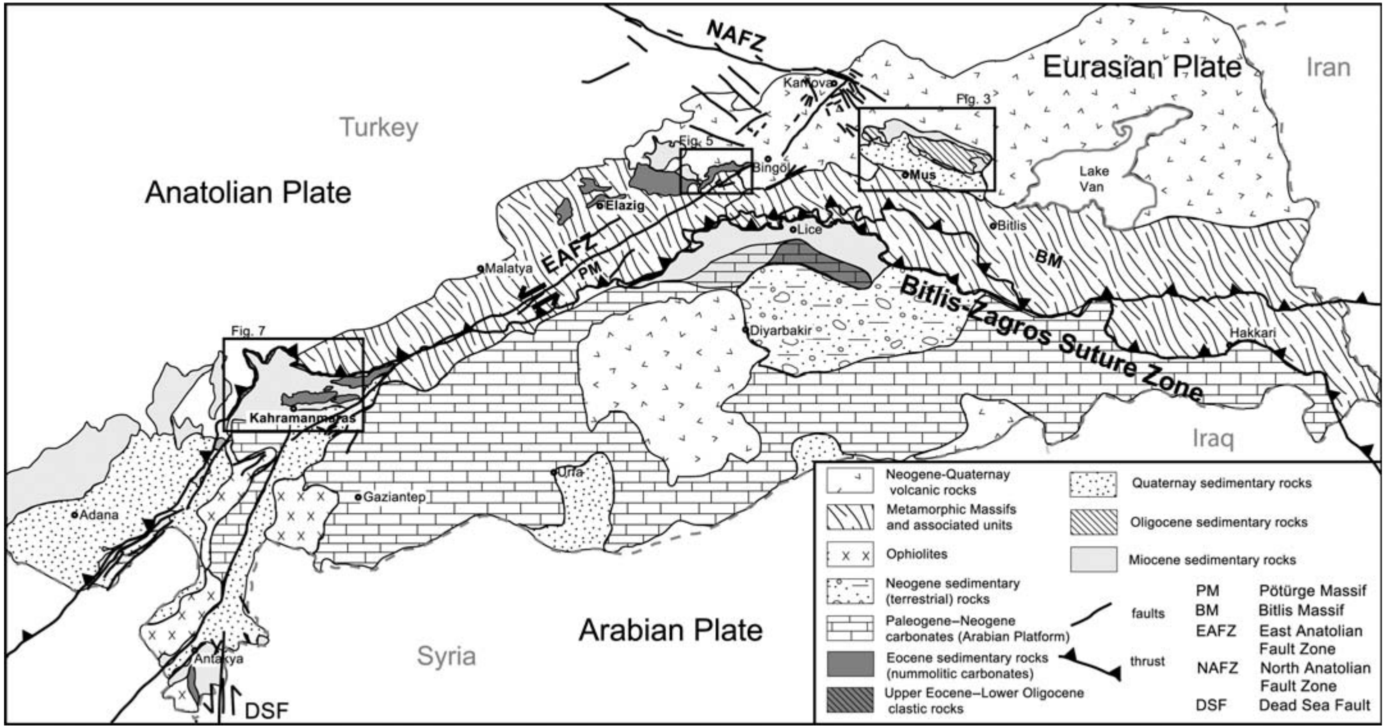

Fig. 2. Outline of schematic geological map of SE Anatolia in Southeastern Turkey with major tectonic structures. Note the three boxes indicating the studied areas: Muş in the easternmost part and Elazığ, both north of the Bitlis–Zagros Suture zone and Kahramanmaraş south of the Bitlis–Zagros Suture Zone (drawn after Geological map of Turkey (Şenel 2002)).

between the two continental crusts, Eurasia and African–Arabian. The massif was stacked to form a nappe complex during the closure of the Neo-Tethys by the middle Miocene (Dewey 1986 and references herein).

We have studied the southernmost flysch deposits in the eastern Anatolian orogenic system. These are found in the Muş and Elazığ basins, both north of the Bitlis–Pötürge Massif, and the Kahramanmaraş basin located south of the Bitlis–Pötürge Massif and near the triple junction of the Arabian, Eurasian and Anatolian plates (Fig. 2).

Geological setting of the Muş basin

The Muş basin is an elongated structure located north of the Bitlis–Pötürge Massif and east of the North and East Anatolian Fault (Figs 2 & 3). According to previous studies (Şaroğlu & Yılmaz 1986; Sancay *et al.* 2006) the basin contains upper Eocene to lower Miocene limestones, marls and turbiditic sandstones with marine sedimentation continuous from the Oligocene to Aquitanian. These deposits overlay an upper Cretaceous ophiolitic mélange. Şaroğlu & Yılmaz (1986) suggested that lower Miocene limestones are widespread in the northern part of the Muş area, while middle Miocene strata were not found. These sequences are unconformably covered by allegedly upper Miocene and younger continental clastics and volcanics (Şaroğlu & Yılmaz 1986; Sancay *et al.* 2006). Detailed biostratigraphy was carried out mainly based on dinoflagellates and palynomorphs yielding a Rupelian (early Oligocene) to Aquitanian (early Miocene) age (Sancay *et al.* 2006). The occurrence of the benthic foraminiferal family of *Miogypsinidae* was interpreted as possible indicator for a connection with the Indo-Pacific during the Oligocene (Sancay *et al.* 2006).

We sampled two sections in the Muş basin (Fig. 3). The eastern transect comprises allegedly Eocene–Oligocene clastics in the northern part of the basin, and Oligocene flysch sediments followed by marine limestones which are covered by volcanics. The second transect in the western part of the basin covers the transition from marls to limestones, assuming it is equivalent to the uppermost part of the eastern succession. The entire succession gently dips towards the NW.

The base of the eastern section (east transect in Fig. 3) is determined by a thrust zone emplacing allegedly Eocene clastic sediments onto Pliocene deposits (see geological map of Turkey, Şenel 2002) (Fig. 3). The first 20 m of the studied section is characterized by an alternation of conglomerates, clays, sands, and silts (Fig. 4). A layer of limestone (1.5 m) with shell fragments and the presence of large gastropods clearly indicate shallow

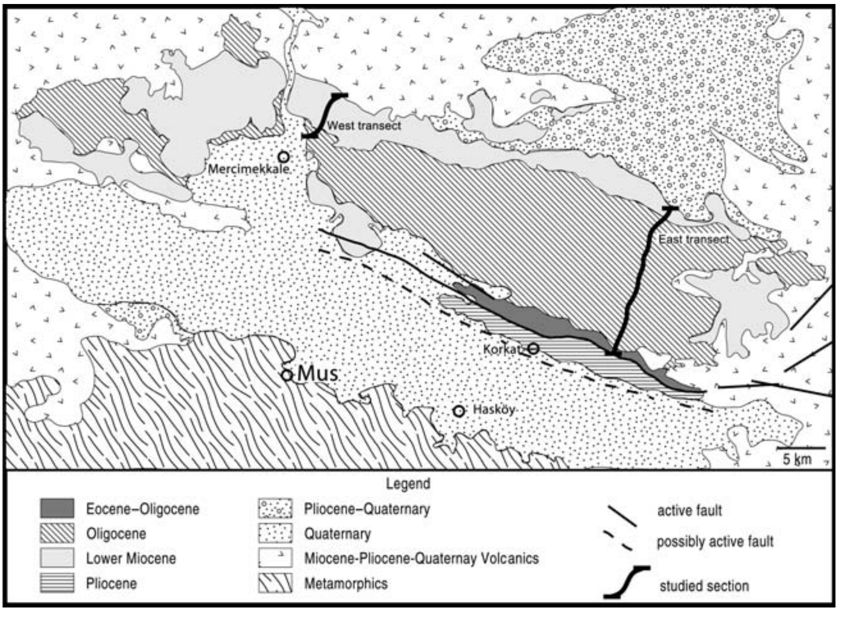

Fig. 3. Simplified tectonic and geological map of the Muş area including the trajectories of the two studied sections: an about 1.4 km long transect in the eastern part of the basin and additionally an about 500 m long transect in the western part of the basin equivalent to the uppermost part of the western transect. Refer to Legend for key to lithology and/or age of outcrops (drawn after Geological map of Turkey (Şenel 2002)).

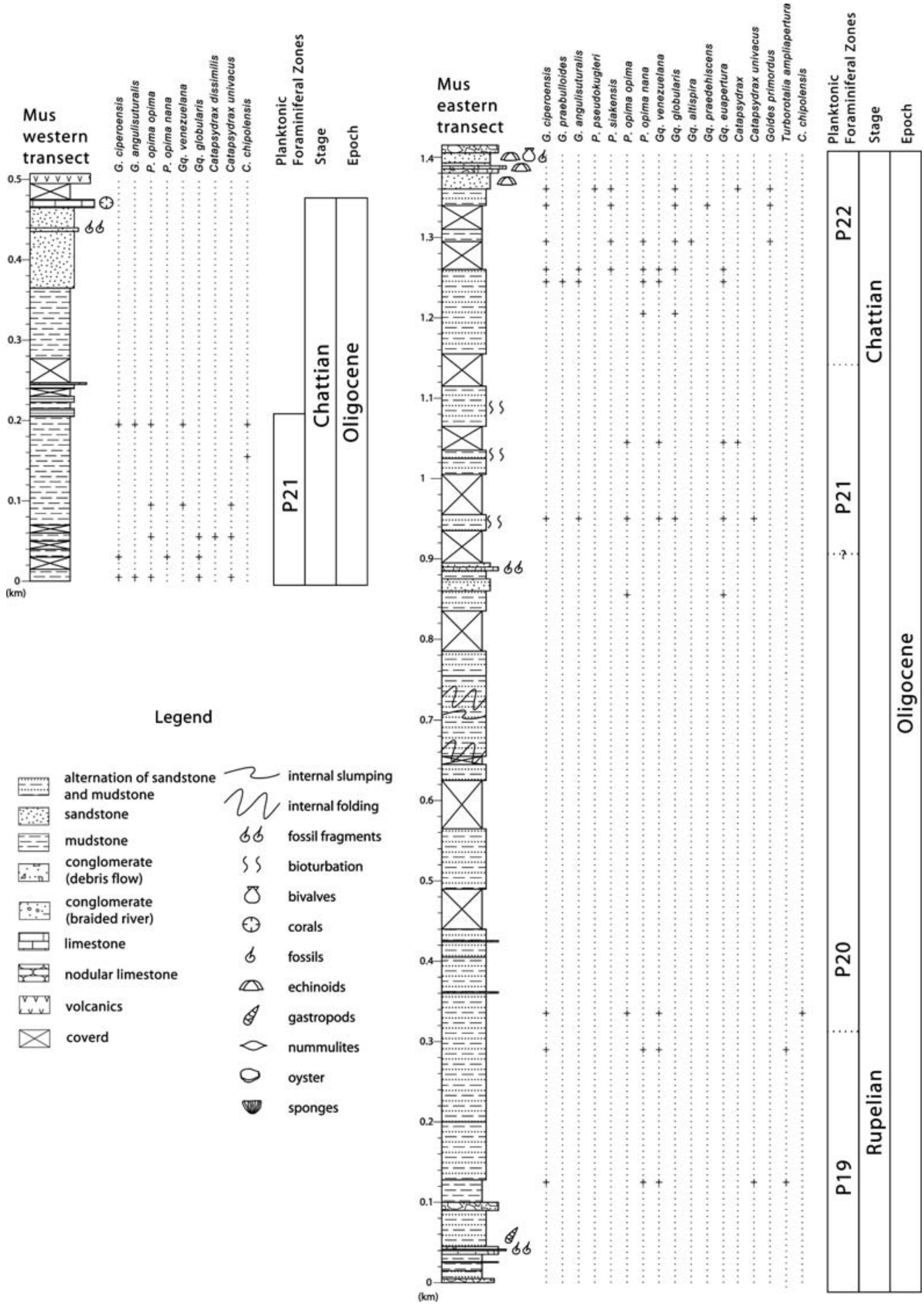

Fig. 4. Lithological column of the studied sections in the Muş basin with the biostratigraphic results. The age model is based on planktonic foraminifer occurrences and the macrofossil assemblage in the uppermost 40 m (mainly limestones and sands) of the stratigraphy. Planktonic foraminifer occurrences have been correlated to planktonic foraminifer zones, which, in turn, are tied to stages during the Oligocene leading to a correlation to the Geological Time Scale. See legend for key to lithologies, structures and fossils.

marine conditions. This sequence is followed by a thick (about 1.3 km) succession of alternating clay and sandstone. Occasionally conglomeratic layers, characterized by angular, unsorted material, occur in the succession. These layers have thicknesses of up to 10 m and are interpreted as debris flows. The sandstone layers show typical transport characteristics such as fining upwards, Bouma sequence, flute casts and fossil fragments indicating a turbiditic origin. These turbidites occur as massive sandstone layers of thicknesses of up to 15 m or as several thinner (up to 50 cm) turbidite layers, probably representing individual events. Only minor slumping, indicating an unstable submarine paleoslope, and folding occur throughout the succession. The upper part of the section shows shoaling characterized by shallow marine limestone, containing echinoderms, bivalves and gastropods, followed by continental clastics.

The western transect (west transect in Fig. 3) is dominated by bluish clay with occasional red sediments. This is followed by a thick, about 100 m, sequence of alternating softer bluish sands, brownish sands and indurate bluish sands, probably all of marine origin. These sediments are overlain by coral limestones, which, in turn, are covered by volcanic rocks, probably of Miocene age. This succession also clearly indicates shoaling towards the top.

Biostratigraphic results of the Muş basin

For biostratigraphy, samples were collected at about every 20 m from both the western and eastern transect (Fig. 3). Not every sample proved to be useful for biostratigraphy or paleobathymetry. The number of foraminifers is extremely variable and most likely fluctuate in pace with changes in terrigenous clastic input. Preservation is generally poor with specimens mostly recrystallized and frequently distorted. Samples from the upper 300 m of the western section are barren in planktonic foraminifers.

The low diversity in planktonic foraminiferal fauna in both sections is dominated by globoquadrinids and catapsydracids with occasional occurrences of *Globigerina ciperoensis* and *Globigerina angulisuturalis* and clearly points to an Oligocene age for the eastern and lower western section (Fig. 4) (Berger & Miller 1988; Spezzaferri & Premoli Silva 1991).

The basal part of the eastern section correlates to planktonic foraminiferal biozone P19 of Berger & Miller (1988) on the basis of trace occurrences of specimens identical to *Turborotalia ampliapertura*. This biozone is Rupelian (early Oligocene) in age (Fig. 4) (Berggren *et al.* 1995). The lowermost occurrence of *Globigerina angulisuturalis* is recorded at 950 m (TR 221) in the eastern section which together with the highest occurrence of *Paragloborotalia opima opima* (at 1045 m (TR222)) indicates that the middle part of the Muş section correlates to planktonic foraminiferal biozone P21 of Blow (1969) and Berger & Miller (1988) which is latest Rupelian to early Chattian in age (Berggren *et al.* 1995). The absence of *Paragloborotalia opima opima* from sample level 1045 m (TR 222) upward in the eastern transect and the occurrence of typical *Paragloborotalia pseudokugleri* and even of forms transitional between *Paragloborotalia pseudokugleri* and *Paragloborotalia kugleri* at the top of the section (1360 m (TR 232)) indicate that the upper part extends upwards into the lower part of planktonic foraminiferal biozone P22 of Berger & Miller (1988) being Chattian in age (Berggren *et al.* 1995). This is confirmed by the presence of *Paragloborotalia siakensis* and *Globigerinoides primordius* in the youngest samples. Both species make their first appearance in the lower part of biozone P22 together with *Paragloborotalia pseudokugleri* (Berger & Miller 1988; Spezzaferri 1994).

In the western section, the co-occurrence of *Globigerina angulisuturalis* and *Paragloborotalia opima opima* at 2 m and 195 m (TR 202 and TR 210) indicates that the lower 200 m correlates to the interval between 900 and 1100 m in the eastern section. Both these intervals belong to biozone P21. This interval is followed by sediments that are barren in planktonic foraminifers but relatively rich in shallow water benthic foraminifers.

The macrofossil assemblage of the uppermost 40 m in the eastern transect comprises bivalves, gastropods and echinoids. The assemblage is diminished by complete aragonite leaching. Nevertheless, the fauna is age indicative and allows palaeoecological interpretations. The mollusc fauna comprises typical Oligocene taxa such as the gastropod *Ampullinopsis crassatina* (Lamarck 1804) and the bivalves *Amussiopecten labadyei* (d'Archiac & Haime 1853) and *Ringicardium buekkianum* (Telegdi-Roth 1914). Some species such as *Dilatilabrum sublatissimus* (d'Orbigny 1852), *Strombus* cf. *praecedens* Schaffer 1912, *Cordiopsis incrassatus* (Nyst 1836), *Amussiopecten subpleuronectes* (d'Orbigny 1852), and *Hyotissa hyotis* (Linnæus 1758) appear during the Chattian and persist into the Miocene.

An important biostratigraphic feature is the co-occurrence of the pectinids *Amussiopecten labadyei* and *A. subpleuronectes* and the occurrence of transitional morphs. This evolutionary phase is recorded so far only from the upper Chattian (Mandic 2000). Especially in the Iranian Qom Basin, this assemblage co-occurs with the larger foraminifera *Eulepidina dilatata*. The last occurrence of *Amussiopecten labadyei* precedes the first occurrence of *Miogypsinoides* which roughly coincides with the base of the early Miocene. The entire mollusc assemblage is therefore pointing to a late Chattian age. This dating is supported by the echinoid fauna. *Parascutella subrotundaeformis* (Schauroth 1865), a sand dollar which occurs most commonly in Northern Italy, is restricted to the Chattian and Aquitanian.

Comparable assemblages are described from the upper Chattian of the central Iranian Qom Formation (Mandic 2000; Harzhauser 2004; Reuter *et al.* 2007) and along the entire northern coast of the Western Tethys (Harzhauser *et al.* 2002). A relation to the Central Paratethys is indicated by the occurrence of *Ringicardium buekkianum*, which is known from the Lower Egerian (Upper Chattian) deposits of Hungary (Báldi 1973). The faunistic relations towards the east are low. Only *Dilatilabrum sublatissimus* (d'Orbigny 1852) reaches to the Zagros Basin and the Arabian shelf during the Aquitanian (Harzhauser *et al.* 2007). The echinoderm *Clypeaster waageni* (Duncan & Sladen 1883), in contrast, represents ties with the echinoid fauna of the Lower Indus Basin.

Numerical ages for the basin fill are provided by three planktonic foraminiferal bioevents. However, equating highest and lowest occurrences (ho and lo) with the Last Occurrence (LO) and First Occurrence (FO) of theses species should be accepted with reservation because the positions are poorly delineated due to large sampling distances in combination with scarcity and poor preservation of the age diagnostic species.

The oldest bioevent in the Muş section is the lowest occurrence of *Turborotalia ampliapertura* some 300 m above the base of the eastern section (TR 190). The LO of this species is calibrated at 30.3 Ma (Berggren *et al.* 1995) providing a minimum age for the base of the Muş section. The age for the top of the eastern section should be slightly younger than the age of 25.9 Ma for the FO of *Paragloborotalia pseudokugleri* (Berggren *et al.* 1995) because of the presence of paragloborotalids being transitional between *Paragloborotalia pseudokugleri* and *Paragloborotalia kugleri*. The ho of *Paragloborotalia opima opima* at 1045 m (TR 222) in the eastern section provides an extra age calibration point of 27.456 Ma being the calibrated age for the LO of *Paragloborotalia opima opima* at ODP Site 1218 (Wade *et al.* 2007). The dating of the top of the section is in accordance with the macrofauna which strongly indicates a late Chattian age for the upper 40 m the eastern transect.

No numerical ages are provided for the western section. However, based on the co-occurrence of *Globigerina angulisuturalis* and *Paragloborotalia opima opima* in the lower 200 m, this interval correlates to the biozone P21. The upper 300 m lack any age diagnostic planktonic foraminifer.

Palaeoenvironmental interpretations for the Muş basin

Benthic foraminifers in the sections were furthermore used to estimate the depositional depth. The commonly used method of calculating depth by determining the ratio between planktonic and benthic foraminifers (van der Zwaan *et al.* 1990; van Hinsbergen *et al.* 2005*b*) is not reliable here due to significant downslope transport (seen in presence of notorious epifytes and shallow water benthic foraminifers such as *Pararotalia* and *Amphistegina*) and poor preservation. Instead, we focus on the deepest water benthic foraminiferal depth markers (for list see van Hinsbergen *et al.* 2005*b*) and the macrofossils. In the eastern section, the depositional environment of the lower 20 m is characterized by shallow marine conditions, indicated by shell fragments in the limestone. However, a rapid deepening trend occurs at about 50 m indicated by the presence of benthic foraminiferal depth markers (typically *Cibicides (pseudo) ungerianus*, *Gyroidina* spp. *Uvigerina* spp. and occasionally *Oridorsalis* spp.), and the absence of markers for deeper water, which points at a depositional depth range of 350 to 750 m (the upper limit is constraint by the occurrence of *Oridorsalis* spp. after van Hinsbergen *et al.* 2005*b*). Towards the top of the eastern section rapid shoaling is evident from the presence of macrofossils. Both the molluscs and echinoderms of the uppermost 40 m indicate a shallow marine, tropical to subtropical, depositional environment with sand bottoms and algal or sea grass patches. Giant conchs such as *Dilatilabrum sublatissimus* (d'Orbigny 1852) are found today in sea grass meadows and sheltered lagoons, where they live partly buried in the soft substrate (Bandel & Wedler 1987). Similarly, the extant representatives of the oyster *Hyotissa hyotis* prefer shallow subtidal habitats where they are attached to rocks and corals (Slack-Smith 1998). Extant *Echinolampas* and *Clypeaste*r, too, occur most commonly on sandy sediments with sea grass patches (Hendler *et al.* 1995).

In the western section a shoaling trend in the upper 250 m is observed by the relatively rich occurrence of shallow water benthic foraminifers and occasional red sediments. The differences between west and east suggest that the western part of the Muş basin shoaled more rapidly or earlier during the Chattian than the eastern part.

Implications for the Muş basin

Based on the occurrence of turbidites, slumping and minor folding, this about 1.5 km thick marine succession is interpreted as deposits of a deep marine basin.

Shallow marine conditions during the Rupelian (P19) were replaced by rapid deepening of the basin during biozone P22, late Chattian. The end of the flysch deposition during the Chattian marks the emergence of the basin which probably remained shallow marine until the late Chattian.

Considering the biostratigraphic ages, a sedimentation rate between 15 and 27 $^{cm}/_{ka}$ is calculated. The constant water depth of 350 to 750 m during deposition indicates approximately 2 km of subsidence throughout the Oligocene, followed by rapid uplift and exposure of the succession after the late Chattian. Our biostratigraphic dates based on planktonic foraminifers in the flysch deposits corroborate the ages published previously based on dinoflagellates and palynomorphs (Sancay *et al.* 2006).

Geological setting of the Elazığ basin

The studied Gevla section is situated in the easternmost part of the Elazığ basin, about 40 km NE of Elazığ (Fig. 2). The basin has been studied by several workers; however, the literature has been published mostly in Turkish (see Aksoy *et al.* 2005) and no detailed information is available for the easternmost part of the basin. At present, the basin fill is exposed in an NE–SW belt in the eastern Taurides of Anatolia. The generalized stratigraphy of the Tertiary sediments has been described as: lower Paleocene continental deposits at the base, followed by upper Paleocene to lower Miocene marine deposits and finally Pliocene to Quaternary continental deposits. The basement of the Elazığ basin is formed by Permo-Triassic metamorphic rocks, namely Keban Metamorphics, which were emplaced over upper Cretaceous magmatic rocks north of Elazığ (Perinçek 1979; Perinçek & Özkaya 1981; Aktaş & Robertson 1984; Bingöl 1984; Aksoy *et al.* 2005).

Detailed stratigraphic, sedimentological and tectonic characteristics of the Elazığ area have been discussed elsewhere (e.g. Perinçek 1979; Perinçek & Özkaya 1981; Aktaş & Robertson 1984; Bingöl 1984; Cronin *et al.* 2000*a*, *b*; Aksoy *et al.* 2005). From the late Paleocene, shallow marine carbonates, deposited in an extensional back-arc setting, were accumulated when the basin further subsided until Middle to Late Eocene (Aksoy *et al.* 2005). During Oligocene to early Miocene, after reaching its maximum extend during the Middle to Late Eocene, deposition was restricted to the N–NW and became progressively shallower, indicated by Oligocene reefal limestones until the final subaerial exposure at the end of Oligocene. Marine Miocene deposits are restricted to small areas in the basin and more widespread north of the basin. From Middle Miocene onwards the basin was affected by a strong, north–south, compression. Later, Pliocene to Pleistocene alluvial fan, fluvial and lacustrine sediments were deposited covering Early Miocene sediments (Cronin *et al.* 2000*a*, *b*; Aksoy *et al.* 2005).

In this setting, we studied a section situated in the easternmost part of the Elazığ basin. According to the geological map of Turkey (Şenel 2002), in the area east of the town Basyurt (Fig. 5), Lower to Middle Eocene continental clastics unconformably overly Mesozoic ophiolitic mélange. These clastic sediments are, in turn, overlain by either Miocene–Pliocene clastic or volcanic rocks.

The basal part of the studied Gevla succession, about 15 km NE of Basyurt, starts with bluish marine clay containing bivalves, followed by an alternation of clay and sandstone (the sandstones are up to 50 cm thick or about 5 m thick with cross bedding) (Fig. 6). A distinct layer with abundant bivalves and gastropods is located at about 50 m stratigraphic position. Three distinct limestone layers occur between about 100 m and 260 m stratigraphic level. The first one, at about 100 m, is a nodular limestone with shell fragments, sponges (up to 30 cm) and corals, followed by two nummulitic limestone horizons, at 244 m and 255 m. This is followed by about 400 m of blue clay grading into a 600 m thick succession of alternating clay and sandstone, whereby the sand layers show typical transport characteristics, such as shell fragments,

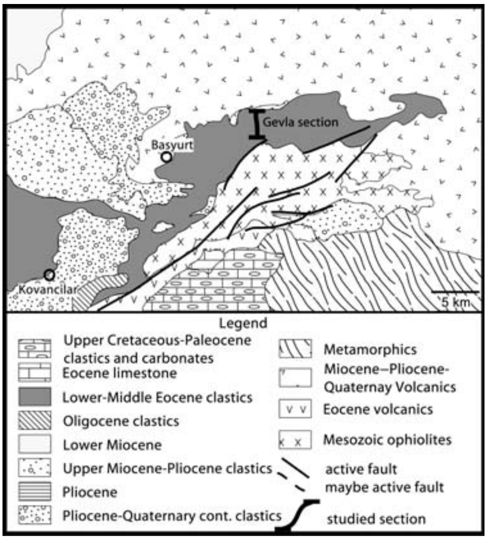

Fig. 5. Simplified tectonic and geological map of the easternmost part of the Elazığ basin. The trajectory of the studied section, called Gevla, is about 15 km NE of the city Basyurt and covers the interval between Eocene limestones and Miocene volcanics to the north. For key to the lithologies and/or ages refer to Legend (drawn after Geological map of Turkey (Şenel 2002)).

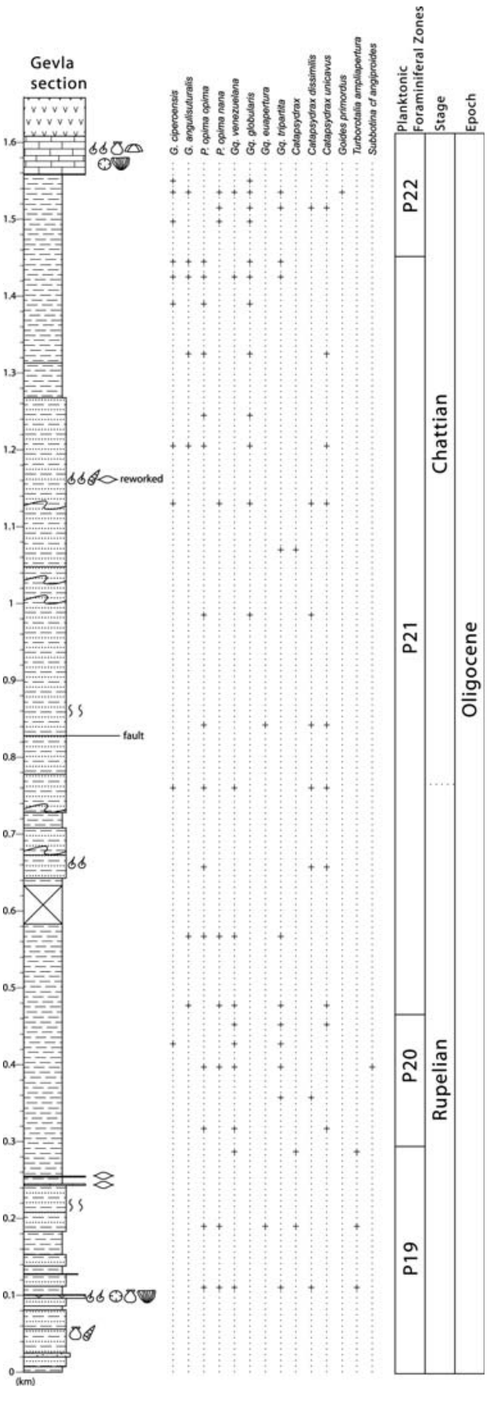

Fig. 6. Lithological column of the studied Gevla section in the Elazığ basin with the biostratigraphic results. The age model is based on planktonic foraminifers and macrofossil assemblage in the 50 m of stratigraphy. Planktonic foraminifer occurrences have been correlated (*Continued*) to planktonic foraminifer zones, which, in turn, are tied to stages during the Oligocene resulting into a correlation to the Geological Time Scale. Refer to Legend in Figure 4 for key to lithologies, structures and fossils.

displaced nummulites and gastropods (for instance at 663 m and 1158 m), fining upward sequences and cross bedding. These layers are interpreted as turbiditic in origin. This succession is followed by about 300 m of blue clay, and the section ends with a 50 m thick limestone with bivalves (up to 5 cm), and clayey intervals with well preserved echinoderms, sponges and corals. These limestones, in turn, are covered by Miocene volcanic rocks. In total, the section is about 1.6 km thick.

Slumping at several levels within the succession indicates an unstable submarine slope. Internal folding is not observed within the succession. The entire succession gently dips towards the NW.

Biostratigraphic results of the Elazığ basin

Hand samples were collected from about every 20 m throughout the entire section, but not every sample contained (diagnostic) planktonic and/or benthic foraminifers. The number of foraminifers is extremely variable and most likely fluctuates with changes in terrigenous clastic input. Preservation is generally poor, with specimens mostly recrystallized and frequently distorted. The overall aspects of the planktonic foraminiferal fauna in this section is similar to that of the Muş section, which means that the foraminiferal fauna is dominated by globoquadrinids and catapsydracids with occasional occurrences of *Globigerina ciperoensis* and *Globigerina angulisuturalis* pointing to an Oligocene age for this section (Fig. 6) (Berger & Miller 1988; Spezzaferri & Premoli Silva 1991). The presence of *Turborotalia ampliapertura* up to and including level 287 m (TR 244) provides evidence that the lower part of the section correlates with planktonic foraminiferal biozone P19 of Berger & Miller (1988), which is late Rupelian, early Oligocene, in age (Berggren *et al.* 1995). The lowest occurrence of *Globigerina angulisuturalis* is recorded at 477 m (TR 250) which in terms of the zonal scheme of Berger & Miller (1988) would mark the top of biozone P20 although it should be noted that *Globigerina angulisuturalis* is neither frequent in this section nor does it display very prominent U-shaped sutures. Typical *Paragloborotalia opima opima* is present from level 317 m (TR 245) up to and including level 1445 m (TR 293) indicating that the larger part of the Gevla section correlates with planktonic foraminiferal biozone

P21 of Blow (1969) and Berggren *et al.* (1995) which in terms of chronostratigraphy is latest Rupelian to early Chattian in age (Berggren *et al.* 1995). The top of the section post-dates the highest occurrence of *Paragloborotalia opima opima*, and correlates to the basal part of the late Chattian planktonic foraminiferal biozone P22 (Berger & Miller 1988), which is evidenced by the joint presence of *Paragloborotalia opima nana*, *Globigerina ciperoensis*, *Globigerina angulisuturalis* and *Globigerinoides primordius*.

The macrofossil assemblage from the upper 50 m in this section is similar to the assemblage in the uppermost 40 m of the eastern transect in the Muş basin (Figs 3 & 4). Both assemblages bear a typical late Chattian pectinid fauna with *Amussiopecten labadyei* and *A. subpleuronectes. Pecten arcuatus* (Brocchi 1814), a widespread Oligocene species, a typical Western Tethys element, is present as well, along with the thin-shelled lucinid bivalve *Anodontia globulosa* (Deshayes, 1830). The dominance of such thin shelled species might indicate a slightly deeper environment than in the corresponding section of the Muş basin, yet not deeper than the medium deep sublittoral environment (Mandic and Piller 2001).

The LO of *Turborotalia ampliapertura* has been calibrated to 30.3 Ma within Chron 11r (Berggren *et al.* 1995). The highest occurrence of this species in level 287 m (TR 244) therefore suggests an age older than 30.3 Ma for the bottom of the section. The LO of *Paragloborotalia opima opima* in level 1445 m (TR 293) has been recently recalibrated to 27.456 Ma within Chron 9n at ODP Site 1218 (Wade *et al.* 2007). This age provides a maximum age for the top of the section since the highest occurrence of *Paragloborotalia opima opima* occurs near the top of the section (TR 293). A correlation of the upper 50 m of the section to biozone P22 is supported by the mollusc fauna which indicates a late Chattian age.

Paleoenvironmental interpretations for the Elazığ basin

The depositional environment during the lower Rupelian (biozone P19) was first shallow marine as indicated by the occurrence of limestone with corals, bivalves and gastropods.

However, the depositional environment rapidly deepened as indicated by benthic foraminiferal depth marker species (*Cibicides* (*pseudo-*)*ungerianus*, *Gyroidina* spp. *Uvigerina* spp. and occasionally *Oridorsalis* spp.). Their presence up to the top indicates that the basin was 350 to 700 m deep during much of the Oligocene. The benthic foraminifers do not give any evidence for shoaling, although the limestone deposits at the top of the section and their macrofossils indicates a medium to shallow subtidal environment for the late Chattian.

Implications for the Elazığ basin

The first 260 m of the studied section was deposited under shallow marine conditions during Rupelian (biozone P19). This was followed by a rapid deepening during the Rupelian and the deposition of about 1.3 km in a relatively deep marine (300 to 750 m) environment. During the late Chattian (biozone P22), the basin experienced rapid shoaling to medium deep sublittoral conditions, preferred conditions for echinoids and bivalves. The inferred late Chattian age of the macrofossils in the top of the section indicates that the final emergence of the basin must have occurred shortly after the Chattian followed by widespread Miocene volcanism.

The numerous internal slumping and sandstone layers, referred to as turbidites, indicate a submarine, unstable slope. The entire succession is interpreted as flysch deposited in a deep marine basin, comparable to the Muş basin. Thus, during the Oligocene, rapid (15–30 $^{cm}/_{ka}$) sedimentation of clay and turbidites dominated the basin evolution.

These new biostratigraphic ages differ significantly from the geological map of Turkey (Şenel 2002) where these sediments are indicated as Lower to Middle Eocene. Our data suggests instead that these sediments were deposited under deep marine conditions during the Oligocene, from the Rupelian until the late Chattian, and, additionally, the shallow marine limestones at the top of the section are late Chattian in age. This data also differs from previous studies in the area (e.g. see Aksoy *et al.* 2005 for a compilation of data from the Elazığ basin) where the Eocene time has been identified as the main period of deep marine deposition and in the Oligocene time shallow marine deposits were restricted to the NW of the Elazığ basin. Our data however indicates that at least the eastern part of the Elazığ basin was deep marine throughout the Oligocene and shoaled and emerged only in the late Chattian, latest Oligocene.

Geological setting of the Kahramanmaraş basin

The Kahramanmaraş basin is located near the triple junction of the Arabian, African and Anatolian plates. As a result of the collision of Arabia and Eurasia along the Bitlis Suture a trough formed in front of the thrust sheets and was consequently filled by thick alluvial sediments and thick turbiditic flysch sequences (Lice Formation) (Şengör & Yılmaz 1981; Perinçek & Kozlu 1983; Karig & Kozlu 1990;

Yılmaz 1993). According to several studies (Perinçek 1979; Perinçek & Kozlu 1983), the Kahramanmaraş basin was part of this elongated foreland basin extending from Hakkari in southeastern Turkey, close to the border to Iran and Iraq, to Adana in southern Turkey (Fig. 2). This basin was also called the Lice trough (Dewey *et al.* 1986; Karig & Kozlu 1990; Derman & Atalik 1993; Derman 1999). Eocene deposits in the Kahramanmaraş area are part of the Arabian Platform (Robertson *et al.* 2004). They indicate a shallow marine depositional environment with local terrestrial input followed by allegedly lower to middle Miocene reefal limestone and claystone (Gül *et al.* 2005). Oligocene bioclastic limestones are reported only from the margin of the Kahramanmaraş area (Fig. 7) (Karig & Kozlu 1990). Basal shallow marine red-bed and basalt sequences of the Kalecik Formation have an inferred age of late Burdigalian to Langhian (Karig & Kozlu 1990). The retreat of marine conditions and basin deformation was assumed to have taken place in the late Miocene, although the age control was not documented (Karig & Kozlu 1990).

Three separate sections (Figs 7, 8a & b), all north of the city of Kahramanmaraş, are been studied by us. The lower 200 m were sampled in the hills in the southern part of the main basin (Hill section), the following about 4.6 km along the road north of Kahramanmaraş (Road section) and the upper 1.5 km stratigraphic transect near the village of Avcılar (Avcılar section).

The base of the Hill section consists of nummulitic limestones according to the Geological Map of Turkey (Şenel 2002) of Eocene age, followed by red, conglomeratic sediments with several basalt layers.

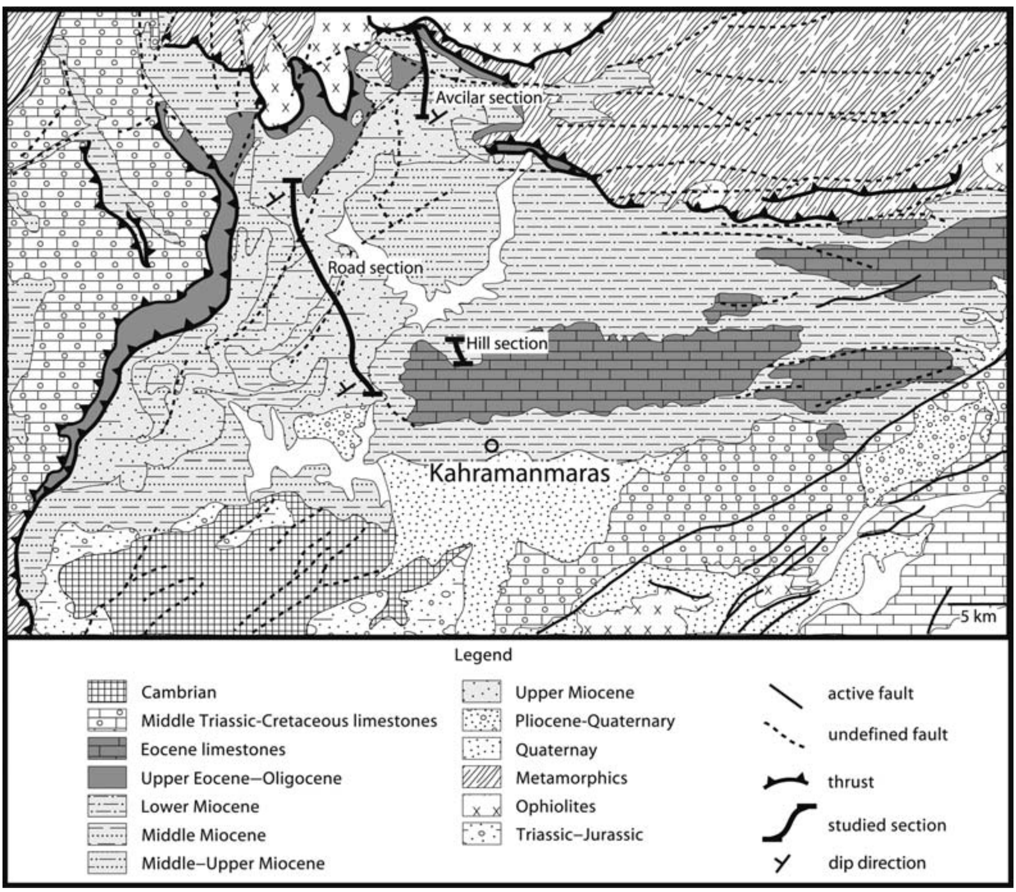

Fig. 7. Simplified tectonic and geological map of the Kahramanmaraş area including the trajectories of the three studied sections north of the city of Kahramanmaraş: (**1**) the lowermost 200 m in the Hill section. (**2**) about 4.6 km of succession along the road (Road section). (**3**) the upper 1.6 km up to the thrust studied in the Avcılar section in the northernmost part of the region. Refer to Legend for key to lithologies and/or ages (drawn after Geological map of Turkey (Şenel 2002)).

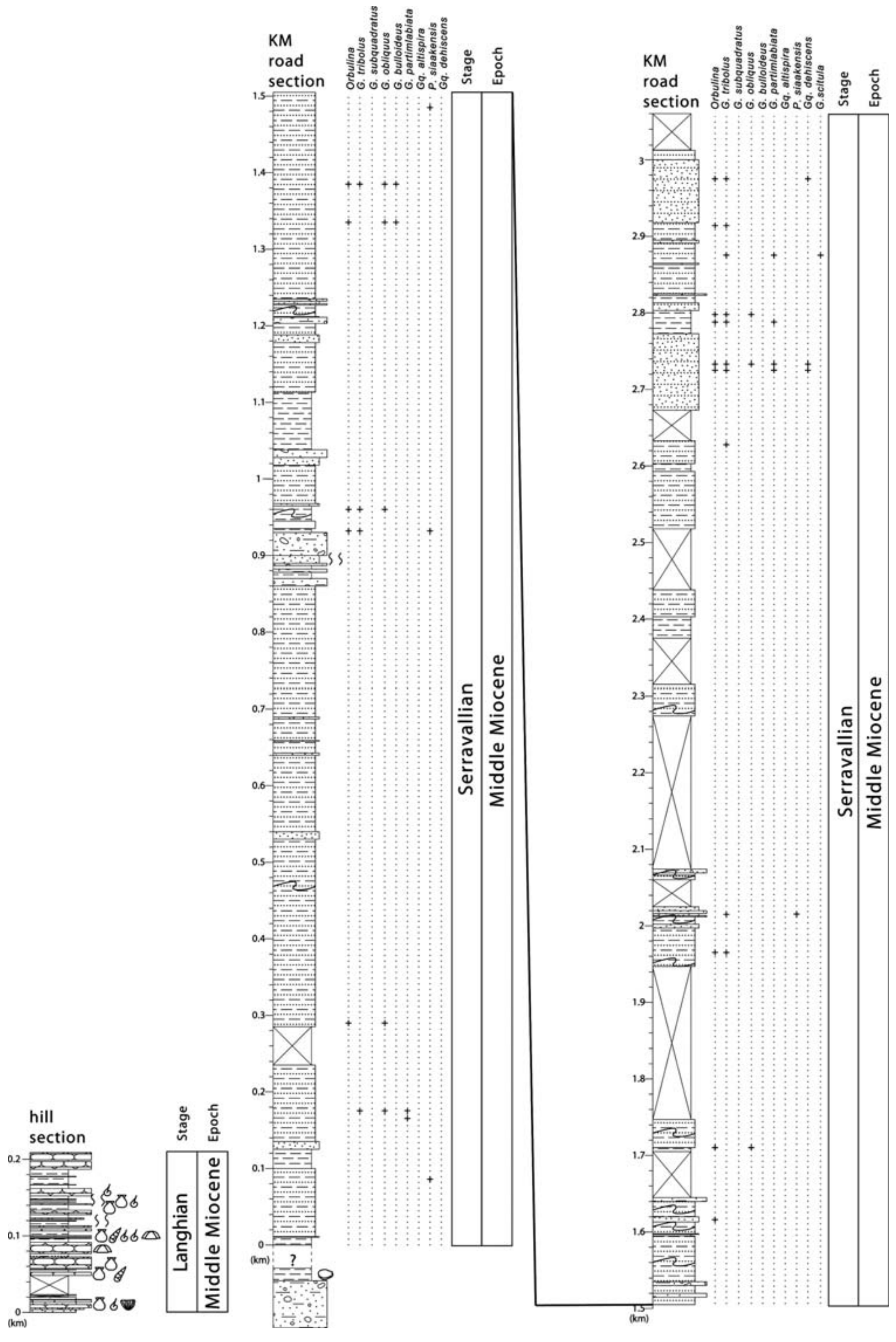

Fig. 8. (**a**) Lithological column of the Hill section and part of the Road section (*c*. 3 km) in the Kahramanmaraş basin with the biostratigraphic results. The age model is based on planktonic foraminifer occurrences, which delineate the correlation of the Hill section to the Langhian and the first *c*. 3 km of the Road section to the Serravallian.

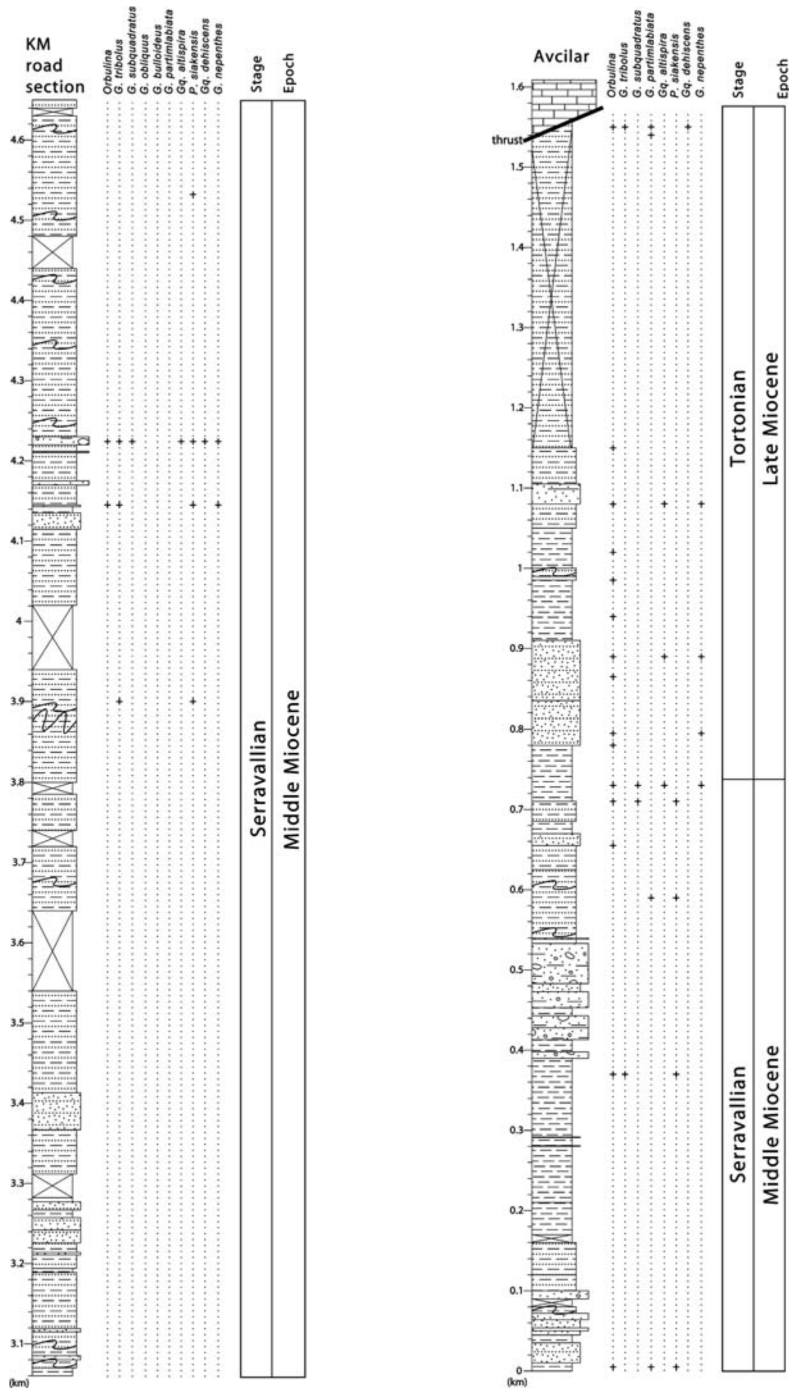

Fig. 8. (*Continued*) (**b**) Lithological column of the upper *c*. 1.6 km of the Road section and the Avcılar section in the Kahramanmaraş basin with the biostratigraphic results. The age model is based on planktonic foraminifer occurrences, which delineate the correlation of the upper *c*. 1.6 km of the Road section to the Serravallian and the lower part of the Avcılar section to the Serravallian, probably overlapping with the Road section, and from *c*. 700 m to the Tortonian based on the LCO 0of *Globigerinoides subquadratus*. Refer to Legend in Figure 4 for key to lithologies, structures and fossils. KM = Kahramanmaraş.

The studied section begins with a 200 m thick succession of nodular limestone (10–15 m thick) alternating with bluish marls. The limestones contain macrofossils such as corals, sponges, echinoderms, bivalves and gastropods, indicating a shallow marine environment. This succession grades into an alternation of marl and sandstones layers, which show typical Bouma sequences and flute casts, which are indicative for a turbiditic origin.

The base of the Road section, however, exposes a strongly different succession, where almost 1 km of the stratigraphy is dominated by large conglomerate lenses. This thick succession of conglomerates contains sand lenses showing cross bedding, indicative of interfingering of braided river channels. This thick fluvial succession probably forms, at least in part, the lateral equivalent of the shallow marine succession in the Hill section. This conglomeratic succession is followed by a level rich in oysters, indicating a transition into shallow marine conditions. This then grades quickly into a very thick succession of alternating marl and sandstone (as mentioned above) with occasional conglomeratic layers, interpreted as debris flows, which cut through the stratigraphy. The sandstones show typical characteristics for turbidites, such as flute casts and Bouma sequences. Some intervals are dominated by massive sandstone layers and/or debris flows, while others are characterized by mainly clay. Slumping can be easily differentiated from (minor) internal folding, both occurring throughout the section. Internal folding, however, does not occur often. The Road section ends at the highest point in the topography along the road going NNW from Kahramanmaraş and since the stratigraphy dips to the NW, a continuation of the stratigraphy was found to the NE, the Avcılar section (Fig. 7). This section was sampled assuming sufficient overlap with the Road section, until the stratigraphy was cut unconformably by carbonates (Figs 8a & b). The stratigraphy of the Avcılar section also consists of a thick succession (about 1.5 km) of mudstone and sandstone with occasional conglomeratic layers, interpreted as debris flows. No shoaling trend based on sedimentological characteristics has been observed towards the top of the section, which ends abruptly with the overthrusting of pre-Neogene carbonates, which were emplaced roughly from North. The upper 400 m were not exposed, except for a few meters just underneath the thrust (Fig. 8b).

Biostratigraphic results of the Kahramanmaraş basin

About every 20 m hand samples were taken for biostratigraphy. Only few samples, however, turned out to be useful for biostratigraphy and/or paleobathymetry. Benthic foraminifers in the lower part of the Kahramanmaraş basin, from the Hill section (Fig. 8a) are dominated by milliolids and representatives of Ammonia, Textularia, Nonion and Elphidium indicating shallow marine (inner shelf) conditions although some samples, at 146, 182 and 198 m (TR 9, 12 and 14), respectively, contain few planktonic foraminifers such as *Globigerinoides trilobus*, *Globigerinoides obliquus* and *Orbulina*. Their presence would indicate that the lower part of the Kahramanmaraş sequence postdates the *Orbulina* datum at 14.74 Ma (Lourens *et al.* 2004). This age assignment is further constraint by the presence of the calcareous nannofossil *Cyclicargolithus abisectus* and rare *Spenolithus heteromorphus* along with the absence of *Helicosphaera ampliaperta*. This assemblage is tentatively assigned to NN5 (Martini 1971) indicating a Langhian age.

Orbulina is common in the samples from the Road section. The rare occurrences of *Globoratalia partimlabiata* in the Road section at 165, 175, 2725, 2788 and 2875 m (TR 20, 21, 71, 73 and 77), respectively, are remarkable because they represent the first recording of this species in Turkey. It has been first described from the middle Miocene of Sicily (Ruggieri & Sprovieri 1970) and since then reported from the Mediterranean (amongst others Foresi *et al.* 1998 and references herein; Hilgen *et al.* 2000; Turco *et al.* 2001; Foresi *et al.* 2002*a*, *b*; Hilgen *et al.* 2003; Abels *et al.* 2005) and adjacent North Atlantic (Chamley *et al.* 1986) and even from the Indian Ocean off NW Australia (Zachariasse 1992). Ages of FO and LO of *Globoratalia partimlabiata* in the Mediterranean have recently been recalibrated at 12.771 and 9.934 Ma (Hüsing *et al.* 2007). Its presence in the basal part of the Road section along with *Globigerinoides subquadratus* at 4224 m (TR 114) indicates that the larger part of the Road section, up to 4200 m, is Serravallian, Middle Miocene, in age, since the base of the Tortonian has been defined at a level close to the Last Common Occurrence (LCO) of *Globigerinoides subquadratus* (Hilgen *et al.* 2000, 2005) with a new astronomical age of 11.625 Ma (Hüsing *et al.* 2007). It cannot be excluded that the Road section terminates into the lowermost Tortonian since *Paragloborotalia siakensis* at 4532 m (TR 120) is the only biostratigraphic marker species present above 4200 m.

In the Avcılar section, the occasional occurrences of *Paragloborotalia siakensis* up to 710 m (TR151) along with *Globorotalia partimlabiata* at 590 m and *Globigerinoides subquadratus* at 710 and 730 m, respectively, (TR 151 and 152) indicate that the lower 700 m of this section is also Serravallian in age. The absence of *Globigerinoides* *subquadratus* and *Paragloborotalia siakensis* in the upper part of the Avcılar section along with the presence of *Globorotalia partimlabiata* near the top of the section (TR 169 and 172) suggests that the section extends up into the Tortonian.

The Avcılar section has been sampled assuming a significant overlap with the Road section and if the uppermost part of the Road section indeed extends into the Tortonian, we might assume an overlap of up to 1 km between these two sections. The maximum age range of the road section and Avcılar section is indicated by the age range of *Globoratalia partimlabiata* of 12.771–9.934 Ma (Hüsing *et al.* 2007).

Paleoenvironmental interpretations for the Kahramanmaraş basin

Deposition of the lower 200 m occurred in shallow marine conditions, as indicated by the occurrence of benthic foraminifers, calcareous nannofossils, poorly preserved echinoderms, gastropods and the large estuarine oyster *Crassostrea gryphoides* (Schlotheim, 1820). This large-sized Oligocene to Miocene species is restricted to brackish water environments with a high nutrient input and prefers building colonies on mud flats of outer estuaries (Slack-Smith 1998). Benthic foraminiferal species of the flysch succession from the road and Avcılar, such as *Cibicides (pseudo-)ungerianus*, *Gyroidina* spp., *Uvigerina* spp., *Oridorsalis* spp. and occasionally *Siphonina reticulata*, suggest water depths between 350 and 750 m during deposition of this section without evidence for shoaling towards the top, which is, in turn, cut by the thrust in the Avcılar section.

Implications for the Kahramanmaraş basin

During the Langhian – early Serravallian, shallow marine conditions prevailed in the Kahramanmaraş basin. The basin deepened during late Langhian/early Serravallian as indicated by the change from limestones and/or conglomerates to an alternation of marl and turbidites. Since neither in the lithology, nor in the biostratigraphic data, a shoaling trend towards the top of the section is observed, deep marine conditions (350–750 m) prevailed in the basin until the early Tortonian.

We interpret the whole section as a characteristic foreland basin flysch succession (as Dewey 1986; Karig & Kozlu 1990; Derman & Atalik 1993; Derman 1999). Assuming the Road and Avcılar sections were sampled with no overlap, the maximum thickness is about 6.1 km, but assuming an overlap of up to 1 km, the maximum thickness is about 5.1 km. It is very difficult to estimate a sedimentation rate for this basin, because three sections were sampled with an unknowing overlap. Secondly the accuracy of the age indicative biostratigraphic events is uncertain due to poor preservation and poor sampling resolution. Furthermore, the age indicative biostratigraphic events, LCO of *Globigerinoides subquadratus* and LO of *Globorotalia partimlabiata* are recorded in different sections, which makes the determination of the sedimentation rate between these two calibration points nearly impossible. The sedimentation rates thus vary much, between 50 and 450 cm/ka, but including slumps, debris flows and turbidites deposited in front of and during the activity of the thrust that now covers the top of the sequence. Taking a conservative estimate of 100 to 200 cm/ka, also because the LO of *Globigerinoides subquadratus* might not correspond to the true LCO, dated at 11.625 Ma (Hüsing *et al.* 2007), but might be higher in the stratigraphy, the age of the youngest flysch is about 11 Ma.

This age range, from Langhian to early Tortonian, differs significantly from the assigned Oligocene age of the open marine flysch and limestone deposits in the Muş and Elazığ basins. The continuous marine sedimentation in the Kahramanmaraş basin from Langhian to early Tortonian at a constant depth indicates that tectonic subsidence, possibly up to the order of 5 km, dominated the evolution of the basin.

Discussion

Evolution of the east Anatolian basins

The stratigraphic results from the east Anatolian basins are summarized in Figure 9, and are correlated to the Geological Time Scale (Gradstein *et al.* 2005). This figure schematically illustrates that the individual basins belong to two different, major basins: (1) a basin north of the Bitlis–Pötürge Massif, encompassing the Elazığ and Muş basins, which was filled with clastic mass flow deposits during the Rupelian and Chattian (Oligocene); (2) a basin south of the Bitlis–Pötürge Massif, a foreland basin which was filled with clastic sediments during the Langhian, Serravallian and early Tortonian (Middle and early Late Miocene).

The Muş and Elazığ basin, both north of the Bitlis–Pötürge Massif, show similar stratigraphic evolution during the Oligocene: Deepening of the basin occurred during the Rupelian and deep marine conditions (350–750 m) prevailed until the Chattian. Both basins evidence a shoaling trend during the Chattian. The macrofossil assemblage in the sandy limestones, such as molluscs and

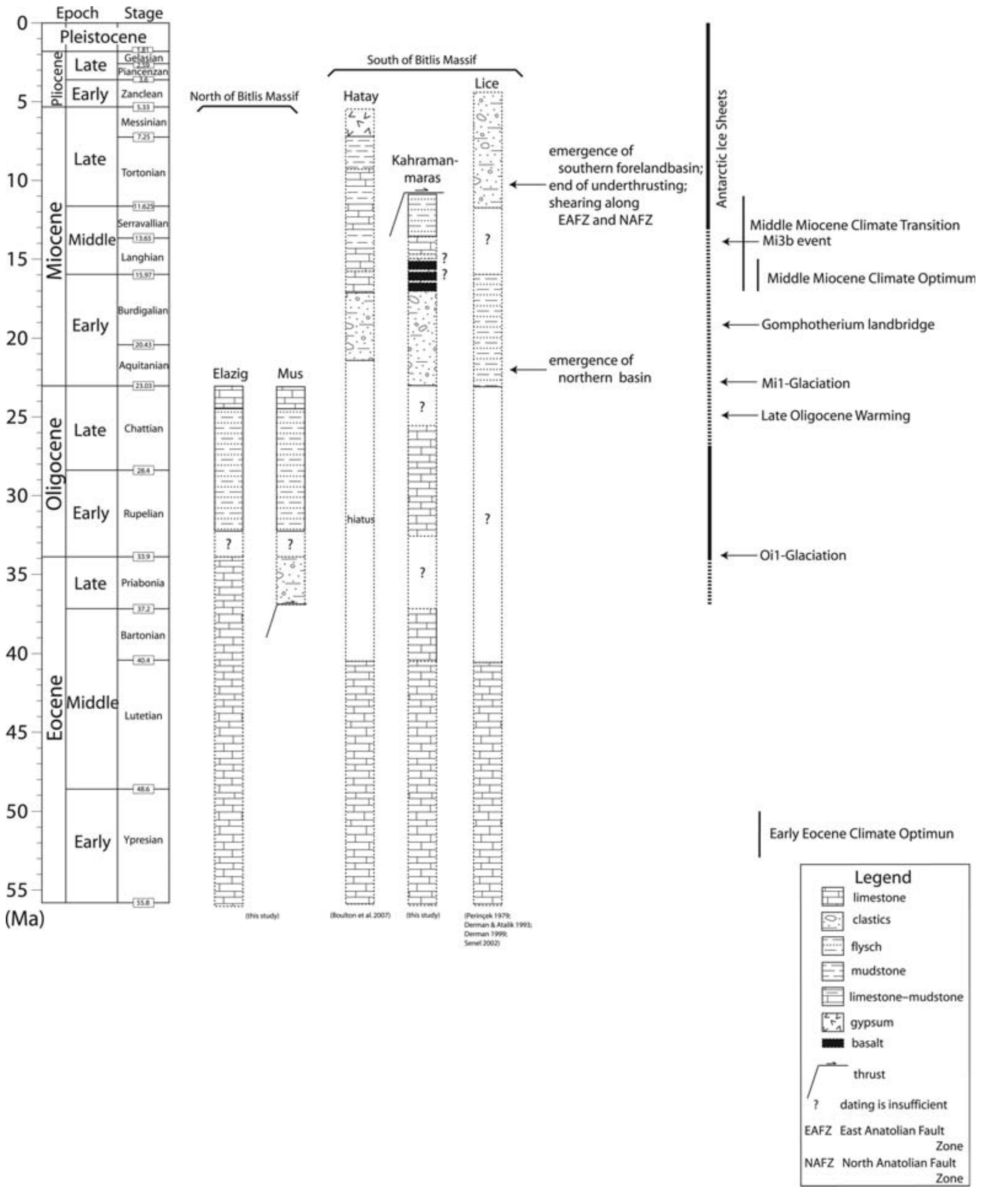

Fig. 9. Chronology of Paleogene–Neogene foreland basin development in Southeastern Turkey. The evolution of the three basins from this study, Muş, Elazığ and Kahramanmaraş, is compared to the Hatay and Lice regions. For purpose of comparison the stratigraphy of all areas has been simplified. Refer to Legend for key to lithologies and structures. Dashed lines of the lithological columns indicate uncertain ages for the section. All ages are given in Ma.

echinoderm, indicates shallow marine, tropical to subtropical deposition, similar to a sheltered lagoon environment, with species preferring subtidal and intertidal environments. In addition, the macrofossil assemblage is comparable to assemblages found in Central Iran, the entire northern coast of the Western Tethys, the Central Paratethys and the lower Indus Ocean, indicating an open marine connection between these marine realms prior to the emergence during the late Chattian. We suggest that the Muş and Elazığ basins were connected forming a large east–west elongated deep marine basin during Rupelian and Chattian.

The rapid deepening of the basin north of the Bitlis Massif may be related either to onset of flexural subsidence associated with (northward) underthrusting within the prevailing overall compressional regime (e.g. for the Elazığ basin Cronin (2000*a*, *b*)) or to the late stages of an extensional deformation period that persisted in the Paleocene and Eocene (e.g. in the Malatya basin (Kaymakçi *et al.* 2006) and in the Muş area (Şengör *et al.* 1985)). These two scenarios are controversial and our data provide age and depth constraints on the Muş and Elazığ basins, which do not allow to eliminate or prefer either of these scenarios.

In the Kahramanmaraş basin, south of the Bitlis–Pötürge Massif, shallow marine sediments were deposited during the Langhian. A rapid deepening during the Langhian to Serravallian indicated by the rapid transition to deep marine (350 to 750 m) flysch deposits, was followed by deposition of continuously deep marine sediments until the early Tortonian. Since no shoaling trend is observed we suggest that the age of the youngest flysch underneath the thrust, biostratigraphically dated as early Tortonian, at about 11 Ma, coincides with the end of underthrusting.

The rapid deepening of the foreland basin south of the Bitlis–Pötürge Massif during the Langhian to Serravallian, followed by the deposition of a thick deep marine flysch succession, can be interpreted as northern Arabia and more specifically the area of the Kahramanmaraş basin, entering into the subduction zone underneath Anatolia. The end of flysch deposition and thus the youngest flysch underneath the thrust of the overriding Bitlis–Pötürge Massif could be envisaged as the end of subduction, thus underthrusting, at about 11 Ma (Tortonian), which is likely followed by rapid uplift in the region. Such episodes of very rapid uplift and folding of foreland basins associated with the stalling of underthrusting is, for example, also well documented in the western Aegean region (Richter *et al.* 1978; van Hinsbergen *et al.* 2005*a*, *c*, *d*).

Our new results of the Kahramanmaraş basin can be compared to previously published data from the Hatay (around Antakya) and Lice regions (see Figs 2 & 9), which have been interpreted as foreland basins related to southward thrusting of the Taurus allochton over the Arabian continental margin belonging to an east–west elongated foreland basin overlying the Arabian promontory (e.g Perinçek 1979; Karig & Kozlu 1990; Derman and Atalik 1993; Derman 1999; Robertson *et al*. 2004).

The stratigraphy and chronology of the Hatay area is very similar to the evolution of the Kahramanmaraş basin. The chronology in the Hatay area has recently been redefined based on micropaleontological dating (Boulton *et al.* 2007) and we can therefore correlate the evolution of the Kahramanmaraş basin to the Hatay area. The stratigraphy in the Hatay area is characterized by a pronounced angular unconformity between middle Eocene and overlying lower Miocene sediments, with a hiatus in the Oligocene (Boulton & Robertson 2007). Sedimentation resumed during the Aquitanian to Burdigalian (Early Miocene) with deposition of conglomerates and mudstones. In the Kahramanmaraş area, Derman & Atalik (1993) and Derman (1999) assigned a lower Miocene age to the about 1 km thick series of fluvial deposits, which precede the thick flysch deposits. We, however, have no age constraints on the fluvial deposits and can therefore not confirm an Early Miocene age. During the Langhian both basins experienced shallow marine limestone deposition and the basin progressively deepened during Serravallian to Tortonian (Boulton *et al.* 2007; Boulton & Robertson 2007). The deposition of shallow marine limestones in the Hatay area have been interpreted to be related to further loading of the lithosphere in response to flexural subsidence and the progressive deepening to flexural control (Boulton & Robertson 2007). Where flexural subsidence exceeded the build up of a carbonate platform hemipelagic sediments were deposited (Boulton *et al.* 2007; Boulton & Robertson 2007). A similar scenario can be envisaged for the Kahramanmaraş basin indicated by coarsening upwards in the thick flysch deposition. In the Hatay area, by the end of the Miocene, the tectonic regime changed and the Pliocene–Quaternary Hatay Graben structure was formed in a transtensional setting related to the EAF (Perinçek & Cemen 1990; Boulton *et al.* 2007; Boulton & Robertson 2007), while deep marine sediments in the Kahramanmaraş basin were overthrusted already during the early Tortonian. This comparison might indicate a diachronous evolution of these two basins with the Kahramanmaraş basin emerging during the Tortonian and the Hatay area remaining open marine until the deposition of Messinian evaporites, or different basin evolutions due to the relatively western position of the Hatay area thus closer to the present-day extent of the eastern Mediterranean.

A comparison to the Lice basin, which is situated to the east of the Kahramanmaraş basin, would evidently give constraints on the syn- or diachronous evolution of the southernmost, Arabian foreland basin. However, the chronology of sediments in the Lice basin is scarcely documented in the literature (e.g. Perinçek 1979; Dewey 1986; Karig & Kozlu 1990; Robertson *et al.* 2004). On the geological map of Turkey (Şenel 2002) shallow marine clastic and carbonatic sediments have been indicated as Early Miocene in age and continental clastic rocks as Middle to Late Miocene in age. This succession would pre-date the flysch deposition in the Kahramanmaraş and Hatay area and would indicate diachronous evolution of the elongated Arabian foreland basin. Other studies assigned, however without documenting an age control, a Tortonian age to the Lice flysch (Dewey 1986). If the flysch deposits in the Lice, Kahramanmaraş and Hatay area are indeed synchronous, we would assume a synchronous evolution of the Arabian foreland basin which emerged during the Tortonian. However since the chronology of the Lice basin is not well documented, firm correlation to the Kahramanmaraş basin and Hatay area remains impossible (see question marks in Fig. 9).

The basin south of the Bitlis–Pötürge Massif including the Kahramanmaraş, Hatay and Lice basins, is interpreted as the southernmost and youngest foreland basin in the east Anatolian fold-and thrustbelt, which formed as a large east–west trending foreland basin on the subducting Arabian plate. The end of underthrusting in the Kahramanmaraş basin is dated at about 11 Ma, but might have been diachronous relative to the emergence of the Hatay and Lice basin.

Tectonic closure of the eastern Tethys gateway

Based on the presented data herein, we envisage the following scenario for the Oligocene to Miocene evolution of the basins north and south of the Bitlis Massif in SE Turkey (Fig. 10). During the early Oligocene, marine sediments were deposited in a large basin to the north of the Bitlis–Pötürge Massif (Fig. 10a). However, our data does not allow us to constrain whether the deepening of

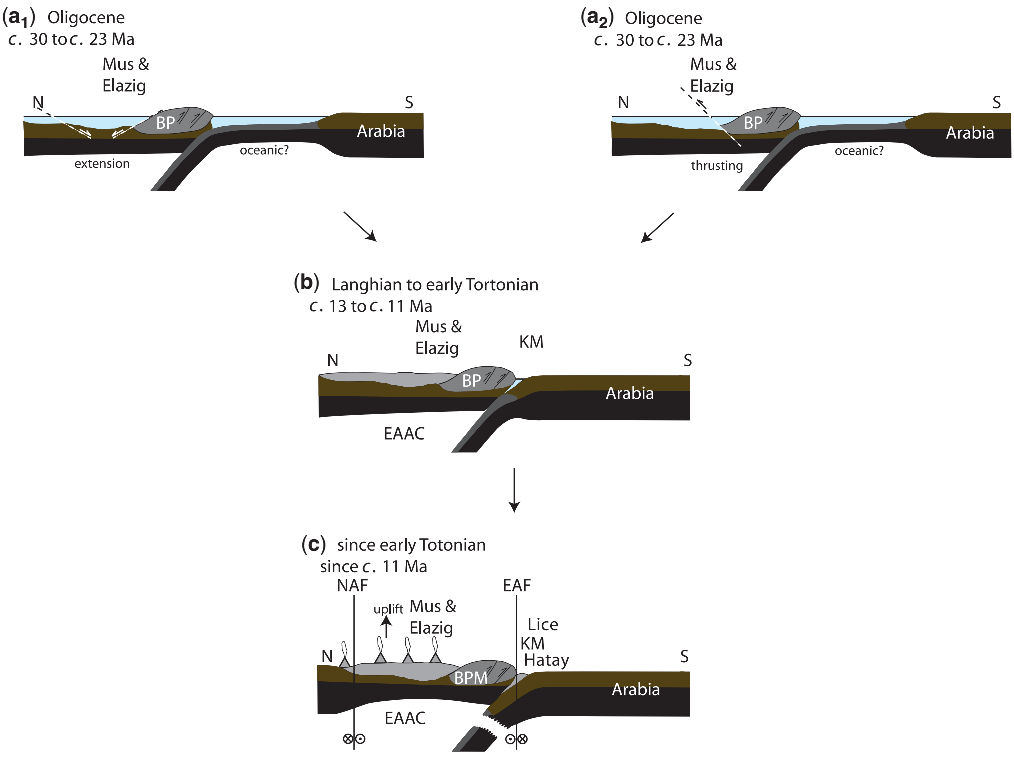

Fig. 10. The evolution of the Oligocene–Miocene basins in SE Turkey are illustrated schematically in three major phases: (**a**) during the Oligocene from *c*. 30 to *c*. 23 Ma: a marine basin was situated north of the Bitlis–Pötürge (BP) until the end of latest Oligocene, Chattian, when this basin emerged; (**a$_1$**) related to extension, (**a$_2$**) related to thrusting. (**b**) during the Langhian to early Tortonian (*c*. 13 to *c*. 11 Ma): areas of present-day northern Arabia enter the position of the foreland basin South of the BP and the northern Arabian promontory was subducted underneath the BP from the Langhian until the early Tortonian, *c*. 11 Ma, and finally. (**c**) since the early Tortonian to Recent: the end of large-scale underthrusting at *c*. 11 Ma in east Anatolia coincides with the onset of collision-related volcanism, uplift of the East Anatolian Accretionary Complex (EAAC), the onset of shearing along the North and East Anatolian Faults (NAF and EAF). Refer to text for further discussion. BP = Bitlis-Pötürge; BPM = Bitlis-Pötürge Massif; NAF = North Anatolian Fault; EAF = East Anatolian Fault; EAAC = East Anatolian Accretionary Complex; KM = Kahramanmaraş.

the basin during the Rupelian was related to either large scale extension (Fig. 10a$_1$) or thrusting (Fig. 10a$_2$), with the Bitlis–Pötürge Massif situated on the overriding plate. Nevertheless, our data suggest that until the Chattian, flysch was deposited in a deep marine environment, as recorded in the area of Muş and Elazığ. The emergence of the basin north of the Bitlis–Pötürge Massif during the late Chattian (see also Fig. 9) probably coincides with the accretion of the Bitlis–Pötürge Massif to the Anatolian plate.

On the southern side of the Bitlis–Pötürge Massif, oceanic subduction was probably ongoing due to Africa/Arabian's relative distal position (e.g. Besse & Courtillot 2002).

During the Langhian to Serravallian the basin south of the Bitlis–Pötürge Massif deepened rapidly, which might be related to the northern Arabian promontory, the present-day northern margin of the Arabian plate (Kahramanmaraş, Hatay and Lice basins), entering into the subduction zone (Fig. 10b) below the Bitlis–Pötürge Massif. During the Serravallian and early Tortonian, the Kahramanmaraş basins remained deep marine indicated by thick flysch deposition until, at least, the early Tortonian. The youngest flysch underneath the thrust in the Kahramanmaraş area, biostratigraphically dated at about 11 Ma, might be linked to the end of the large-scale underthrusting (subduction) in eastern Anatolia (Fig. 10c). In models proposed by Keskin (2003) and Şengör (2003), it is assumed that the Bitlis–Pötürge Massif was accreted with Arabia during late Eocene, while Robertson *et al.* (2004) suggested Late Oligocene–earliest Miocene time. Our data, on the other hand, indicate the presence of a deep marine realm between the Bitlis–Pötürge Massif and Arabia during Serravallian and early Tortonian, which we suggest is associated with the continuous subduction of Arabia underneath the Anatolian plate.

The timing of the end of thrusting agrees with the onset of the collision-related volcanism at about 11 Ma north of the present-day suture line (Keskin 2003), the uplift of the East Anatolian Accretionary Complex inferred to start around 11 Ma onwards (Şengör *et al.* 2003) and the onset of the North and East Anatolian Fault (Dewey 1986; Hubert-Ferrari *et al.* 2002; Şengör *et al.* 2005) (Fig. 10c). Collision-related volcanism and uplift of the East Anatolian High Plateau despite the relatively thin crust (45 km) has been related to an anomalously hot mantle underneath the eastern Anatolia (Keskin 2003; Şengör *et al.* 2003). This, as well as the onset of westward extrusion of Anatolia and the onset of formation of the North and East Anatolian faults, have been explained by slab detachment at about 11 Ma in eastern Anatolia (Keskin 2003; Şengör *et al.* 2003; Şengör *et al.* 2005; Faccenna *et al.* 2006), which is in line with a recent tomography study of Hafkenscheid *et al.* (2006). Our new results from the Kahramanmaraş area can thus be considered in line with the previously suggested scenarios, the end of underthrusting and the onset of extrusion of Anatolia in the Late Miocene (at about 11 Ma) (Fig. 10c).

Constraints on the closure of the eastern Tethys gateway

The continuous northward migration of the African–Arabian plate led to the disruption of the Tethys seaway and the final closure related to continental collision of Arabia and Eurasia. The paleogeographic extent of the Tethys during the Paleogene and Neogene thus underwent significant changes until the connection was finally closed. Several authors suggested that the final closure of the eastern Tethys gateway may have resulted in significant changes in the paleoceanographic circulation and consequently in a major change in global climate (e.g. Woodruff & Savin 1989, 1991; Jacobs *et al.* 1996; Flower & Kennett 1993; Yılmaz 1993).

Our data from eastern Anatolia indicate that a deep marine connection was present north of the Bitlis–Pötürge Massif from Rupelian to late Chattian. The shoaling of this northern basin during the late Chattian led to severe disruption between an eastern (Indian Ocean) and western (Mediterranean) marine domain; particularly the deep-water circulation was disrupted during the Chattian. The emergence of this basin after the late Chattian resulted in the closure of at least this branch of the southern Neotethys and coincides with the late Oligocene warming, reducing the extent of the Antarctic ice, which was punctuated by the Mi-1 glaciations around the Oligocene–Miocene boundary (Zachos *et al.* 2001).

Other studies suggest that the Tethys seaway was open until the early Miocene and became severely restricted during the Burdigalian (*c.* 19 Ma), when mammal fauna and shallow marine macrofaunal records from the eastern Mediterranean region indicate the existence a landbridge (*Gomphotherium* landbridge) connecting Africa/Arabia and Eurasia (Popov 1993; Rögl 1998, 1999; Harzhauser *et al.* 2002, 2007). These authors claim that, since *c.* 19 Ma, biogeographic separation between the Mediterranean-Atlantic and Indo-Pacific regions persisted; despite some short-lived periodic marine connections between the two domains until the middle Miocene (Rögl 1999; Meulenkamp & Sissingh 2003; Golonka 2004; Harzhauser *et al.* 2007). If a causal link between the closure of the eastern Tethys gateway and global climate cooling exists, a major change in global, or at least local, climate must be expected during the Burdigalian time. The most significant climatic change during the Burdigalian, as evidenced in both the δ^{18}O and

$\delta^{13}C$ record, indicates a change from a cooling to a warming trend which led into the Mid-Miocene Climatic Optimum (Zachos *et al.* 2001).

Our data suggest that if a deep marine connection between the eastern and western marine realm persisted after the late Chattian, it was probably located south of the Bitlis–Pötürge Massif. The studied basins along the south Bitlis suture zone in eastern Anatolia, however, do not comprise the stratigraphic interval between late Chattian and Langhian (25–15 Ma). Consequently, it is not possible to constrain the tectonic evolution and the palaeogeographic extent of the Tethys seaway during this time interval from the stratigraphic record of the east Anatolian basins.

In the context of global climate change, the main oxygen and carbon isotope shift corresponds to the second and major step (Mi3b) of the middle Miocene global cooling, and has recently been astronomically dated at 13.82 Ma, close to the Langhian–Serravallian boundary, in a section on Malta (Abels *et al.* 2005). The middle Miocene decrease in $\delta^{18}O$ values was previously attributed, amongst other hypotheses, to a possible local expression of the isolation of the Mediterranean Sea from the Indo-Pacific Ocean (van der Zwaan & Gudjonsson 1986; Jacobs *et al.* 1996). Abels *et al.* (2005), however, show that this event coincides with a period of minimum amplitudes obliquity related to the 1.2-Ma cycle and minimum values of eccentricity as part of both the 400– and 100-ka eccentricity cycle, thus suggesting astronomical forcing (see Abels *et al.* 2005).

If a link between gateway closure and middle Miocene climate change exists, the south Bitlis gateway must have re-opened to finally close in the middle Miocene, which is very unlikely in an overall converging setting. Moreover, our data does not show evidences for a final closure of the seaway in the middle Miocene. In contrast, the data from Kahramanmaraş indicates rapid deepening during the Langhian to Serravallian and prevailing deep marine conditions until the early Tortonian. This has been interpreted as related to continuous northward subduction underneath the Bitlis–Pötürge Massif and finally continental collision during the Serravallian to early Tortonian. Our data suggest that a deep marine connection located between the Bitlis–Pötürge Massif and Arabia, whether periodic or not, was disrupted at latest during the early Tortonian, giving an upper limit of *c.* 11 Ma to the final closure between the Indian Ocean and the Mediterranean along the northern Arabian. The above analysis shows that the end of foreland basin existence in SE Turkey – and therefore the closure of the southern Tethyan gateway – can not straightforwardly be linked to the middle Miocene climate change. Future assessment of the timing of the Tethys gateway closure should focus on detailed stratigraphy of the youngest foreland basins in SE Turkey, NW Iran, Syria and N Iraq, the region of the Bitlis–Zagros suture zone.

Conclusions

The marine basin north of the Bitlis–Pötürge Massif encompassing the Elazığ and Muş basins emerged during Chattian, which was followed by shallow marine limestone deposition during the late Chattian and finally closed after the late Chattian. This marks the disruption of the Tethys gateway north of the Bitlis–Pötürge Massif connecting an eastern (Indian Ocean) and western (Mediterranean Sea) domain.

The Kahramanmaraş basin south of the Bitlis–Pötürge Massif, probably linked to the Hatay and Lice basins, experienced shallow marine conditions during Langhian, rapidly deepened during Langhian to Serravallian and remained deep marine during the Serravallian and early Tortonian. No shoaling trend has been observed in the Kahramanmaraş basin and the age of the youngest flysch underneath the subduction-related thrust has been biostratigraphically dated at early Tortonian, at about 11 Ma. The end of flysch deposition in the Kahramanmaraş area is probably related to the end of subduction, thus the end of underthrusting. The age coincides with the onset of collision-related volcanism, uplift of the East Anatolian Accretionary Complex, and the timing of shearing along the NAF and EAF. Our new results suggest a strong link between the processes outlined above, which have been explained by slab detachment at about 11 Ma in eastern Anatolia.

This age, early Tortonian, about 11 Ma, is the youngest possible age for a deep marine connection between the Mediterranean-Atlantic and Indo-Pacific regions. We can thus constrain the timing of the final closure of a deep marine Tethys gateway to an upper limit of about 11 Ma. The emergence of the basin north of the Bitlis–Pötürge Massif during the late Chattian thus provides a lower limit of the closure of the eastern Tethys gateway.

In the southern basins marine foreland deposition was continuous during Serravallian and early Tortonian and our data does not support a link between the Middle Miocene climate cooling dated at 13.82 Ma and the closure of the eastern Tethys gateway. In contrast, the age of the youngest flysch deposits, thus the youngest foreland basin in SE Turkey is early Tortonian, about 11 Ma.

We thank C. Langereis, N. Kaymakci and E. Yılmaz for their help in the field and M. Triantaphyllou for the determination of nannofossils in the Kahramanmaraş section. We are also grateful for the constructive comments of E. Turco and N. Kaymakci, which led to a significantly improved manuscript. We acknowledge support by the Netherlands Research Centre for Integrated Solid Earth Sciences (ISES) and by the Netherlands Geosciences Foundations (ALW) with financial aid from the Netherlands Organization for Scientific Research (NWO). This work was carried out under the program of the Vening Meinesz Research School of Geodynamics (VMSG) and the Netherlands Research School of Sedimentary Geology (NSG).

References

ABELS, H. A., HILGEN, F. J., KRIJGSMAN, W., KRUK, R. W., RAFFI, I., TURCO, E. & ZACHARIASSE, W. J. 2005. Long-period orbital control on middle Miocene global cooling: Integrated stratigraphy and astronomical tuning of the Blue Clay Formation on Malta. *Paleoceanography*, **20**, 1–17.

AGARD, P., OMRANI, J., JOLIVET, L. & MOUTHEREAU, F. 2005. Convergence history across Zagros (Iran): constraints from collisional and earlier deformation. *International Journal of Earth Sciences*, **94**, 401–419.

AKSOY, E., TÜRKMEN, I. & TURAN, M. 2005. Tectonics and sedimentation in convergent margin basins: an example from the Tertiary Elazig basin, Eastern Turkey. *Journal of Asian Earth Science*, **25**, 459–492.

AKTAŞ, G. & ROBERTSON, A. H. F. 1984. The Maden Complex, SE Turkey: evolution of a Neotethyan active margin. *In*: DIXON, J. E. & ROBERTSON, A. H. F. (eds) *The Geological Evolution of the Eastern Mediterranean*. Blackwell Scientific Publications, Oxford, 375–402.

ALLMENDINGER, R. W., REILINGER, R. & LOVELESS, J. 2007. Strain and rotation rate from GPS in Tibet, Anatolia and the Altiplano. *Tectonics*, **26**, TC3013, doi: 10.1029/2006TC002030.

BÁLDI, T. 1973. *Mollusc fauna of the Hungarian Oligocene (Egerian)*. Budapest, Akadémiai Kiadó.

BANDEL, K. & WEDLER, E. 1987. Hydroid, amphineuran and gastropod zonation in the littoral of the Caribbean Sea, Colombia. *Senckenbergiana maritima*, **19**, 1–130.

BARKA, A. 1992. The North Anatolian fault zone. *Annales Tectonicae*, **6**, 164–195.

BARTOLI, G., SARNTHEIN, M., WEINELT, M., ERLENKEUSER, H., GARBE-SCHÖNBERG, D. & LEA, D. W. 2005. Final closure of Panama and the onset of northern hemisphere glaciation. *Earth and Planetary Science Letters*, **237**, 33–44.

BELLAHSEN, N., FACCENNA, C., FUNICIELLO, F., DANIEL, J.-M. & JOLIVET, L. 2003. Why did Arabia separate from Africa? Insights from 3-D laboratory experiments. *Earth and Planetary Science Letters*, **216**, 365–381.

BERCKHEMER, H. 1977. Some aspects of the evolution of marginal seas deduced from observations in the Aegean region. *In*: MONTADERT, L. (ed.) *Structural History of the Mediterranean Basins*. Technip. Paris, Split, Yugoslavia, 303–313.

BERGER, W. H. & MILLER, K. G. 1988. Paleogene tropical planktonic foraminiferal biostratigraphy and magnetobiostratigraphy. *Micropaleontology*, **34**, 362–380.

BERGGREN, W. A., KENT, D. V., SWISHER III, C. C. & AUBRY, M. P. 1995. A revised Cenozoic Geochronology and Chronostratigraphy. *SEPM Special Publication*, **54**, 129–212.

BESSE, J. & COURTILLOT, V. 2002. Apparent and true polar wander and the geometry of the geomagnetic field over the last 200 Ma. *Journal Geophysical Research*, **107 (B11), 2300**, doi:10.1029/2000JB000050.

BICCHI, E., FERRERO, E. & GONERA, M. 2003. Paleoclimatic interpretation based on Middle Miocene planktonic foraminifera: the Silesia Basin (Paratethys) and Monferrato (Tethys) records. *Paleogeography, Paleoclimatology, Paleoecology*, **196**, 265–303.

BINGÖL, E. 1984. Geology of the Elazig area in the Eastern Taurus region. *In*: *Geology of the Taurus Belt*. MTA (Turkish Geological Survey), Ankara, 209–216.

BLOW, W. H. 1969. Late middle Eocene to Recent planktonic foraminiferal biostratigraphy. *In*: BRONNIMANN, P. & RENZ, H. H. (eds) *Proceedings of the First International Conference on Planktonic Microfossils* (Geneva, 1967), Volume 1: E. J. Brill, Leiden, 199–421.

BOULTON, S. J. & ROBERTSON, A. H. F. 2007. The Miocene of the Hatay area, S Turkey: Transition form the Arabian passive margin to an underfilled foreland basin related to the closure of the Southern Neotethys Ocean. *Sedimentary Geology*, **198**, 93–124.

BOULTON, S. J., ROBERTS, A. H. F., ELLAM, R. M., ŞAFAK, Ü. & ÜNLÜGENÇ, U. C. 2007. Strontium isotopic and micropaleontological dating used to help redefine the stratigraphy of the neotectonic Hatay Graben, Southern Turkey. *Turkish Journal of Earth Sciences*, **16**, 141–179.

BOZKURT, E. 2003. Origin of NE-trending basins in western Turkey. *Geodinamica Acta*, **16**, 61–81.

BROCCHI, G. B. 1814. *Conchiologia fossile subappenina, con osservazioni geologiche sugli Appennini e sul suolo adiacente*. Milano.

CHAMLEY, H., MEULENKAMP, J. E., ZACHARIASSE, W. J. & VAN DER ZWAAN, G. J. 1986. Middle to late Miocene marine ecostratigraphy: clay mineral, planktonic foraminifera and stable isotopes from Sicily. *Oceanological Acta*, **9**, 227–238.

CRONIN, B. T., HARTLEY, A. J., CELIK, H., HURST, A., TÜRKMEN, I. & KEREY, E. 2000*a*. Equilibrium profile development in graded deep-water slopes: Eocene, Eastern Turkey. *Journal of the Geological Society, London*, **157**, 946–955.

CRONIN, B. T., HURST, A., CELIK, H. & TÜRKMEN, I. 2000*b*. Superb exposure of a channel, levee and overbank complex in an ancient deep-water slope environment. *Sedimentary Geology*, **132**, 205–216.

D'ARCHIAC, A. S. & HAIME, J. 1853. *Description des animaux fossiles du groupe nummulitique de l'Inde précédé d'un resumée géologique et d'une monographie de Nummulites*. Gide & Baudry, Paris.

D'ORBIGNY, A. 1852. *Prodrome de Paléontologie Stratigraphique Universelle des Animaux Mollusques & Rayonnés faisant suite au Cours Élémentaire de Paléontologie et de Géologie Stratigraphique*. **2**, Paris, Masson, 1–427.

DERMAN, A. S. 1999. Braided river deposits related to progressive Miocene surface uplift in Kahraman

Maras area, SE Turkey. *Geological Journal*, **34**, 159–174.

Derman, A. S. & Atalik, E. 1993. Sequence Stratigraphic Analysis of Miocene Sediments in Maras Miocene Basin and Effect of Tectonism in the Development of Sequences. *Special Publications Sequence Stratigraphy, Sedimentology Study Group*, **1**, 43–52 [in Turkish].

Deshayes, G.-P. 1824–1837. *Description des coquilles fossiles des environs de Paris. Part I.* Paris.

Dewey, J. F. & Şengör, A. M. C. 1979. Aegean and surrounding regions: Complex multiplate and continuum tectonics in a convergent zone. *Geological Society of America Bulletin*, **90**, 84–92.

Dewey, F. J., Hempton, M. R., Kidd, W. S. F., Şaroğlu, F. & Şengör, A. M. C. 1986. Shortening of continental lithosphere: the neotectonics of eastern Anatolia – a young collision zone, *In*: Coward, M. P. & Ries, A. C. (eds) *Collision Tectonics*, Geological Society, London, Special Publication, **19**, 3–36.

Duncan, P. M. & Sladen, W. P. 1883. The Fossil Echinoidea of Kachh and Kattywar. *Palaeontologia Indica, Ser. XIV*, **1/4**, 1–91.

Faccenna, C., Bellier, O., Martinod, J., Piromallo, C. & Regard, V. 2006. Slab detachment beneath eastern Anatolia: A possible cause for the formation of the North Anatolian Fault. *Earth and Planetary Science Letters*, **242**, 85–97.

Flower, B. P. & Kennett, J. 1993. Middle Miocene Ocean-Climate Transition: High-Resolution Oxygen and Carbon Isotopic Records from Deep Sea Drilling Project Site 558A, Southwest Pacific. *Paleoceanography*, **8**, 811–843.

Flower, B. P. & Kennett, J. P. 1994. The middle Miocene climate transition, East Antarctic ice sheet development, deep ocean circulation and global carbon cycle. *Paleogeography, Paleoclimatology, Paleoecology*, **108**, 537–555.

Foresi, L. M., Iaccarino, S., Mazzei, R. & Salvatorini, G. 1998. New data on calcareous plankton biostratigraphy of the middle-late Miocene (Serravallian/Tortonian) of the Mediterranean area. *Rivista Italiana di Paleontologia e Stratigrafia*, **104**, 95–114.

Foresi, L. M., Bonomo, S., Caruso, A., Di Stefano, E., Salvatorini, G. & Sprovieri, R. 2002*a*. Calcareous plankton high resolution biostratigraphy (foraminifera and nannofossils) of the uppermost Langhian-lower Serravallian 'Ras-il-Pellegrin' section (Malta). *Rivista Italiana di Paleontologia e Stratigrafia*, 337–353.

Foresi, L. M., Caruso, A., Di Stefano, E., Lirer, F., Iaccarino, S., Salvatorini, G. & Sprovieri, R. 2002*b*. High-resolution biostratigraphy of the upper Serravallian/lower Tortonian sequence of the Tremiti Islands. *Rivista Italiana di Paleontologia e Stratigrafia*, **108**, 257–253.

Garfunkel, Z. 1998. Constrains on the origin and history of the Eastern Mediterranean basin. *Tectonophysics*, **298**, 5–35.

Garfunkel, Z. 2004. Origin of the Eastern Mediterranean basin: a re-evaluation. *Tectonophysics*, **391**, 11–34.

Golonka, J. 2004. Plate tectonic evolution of the southern margin of Eurasia in the Mesozoic and Cenozoic. *Tectonophysics*, **381**, 235–273.

Gradstein, F. M., Ogg, J. G. & Smith, A. G. (eds) 2005. *A Geological Time Scale 2004*. Cambridge University Press.

Gül, M., Darbas, G. & Gürbüs, K. 2005. Tectono-Stratigraphic position of Alacik Formation (Latest Middle Eocene – Early Miocene) in the Kahraman Maras Basin. In Turkish with English abstract and summary. *Istanbul University Mühendislik Fakültesi Yerbilimleri Dergisi*, **18**, 183–197.

Hafkenscheid, E., Wortel, M. J. R. & Spakman, W. 2006. Subduction history of the Tethyan region derived from seismic tomography and tectonic reconstructions. *Journal Geophysical Research*, **111**, doi: 10.1029/2005JB003791.

Harzhauser, M. 2004. Oligocene Gastropod Faunas of the Eastern Mediterranean (Mesohellinic Trough/Greece and Esfahan-Sirjan Basin/Central Iran). *Courier Forschungsinstitut Senckenberg*, **248**, 93–181.

Harzhauser, M., Kroh, A., Mandic, O., Piller, W. E., Göhlich, U., Reuter, M. & Berning, B. 2007. Biogeographic responses to geodynamics: A key study all around the Oligo-Miocene Tethyan Seaway. *Zoologischer Anzeiger*, doi: 10.1016/j.jcz.2007.05.001.

Harzhauser, M., Piller, W. E. & Steininger, F. F. 2002. Circum-Mediterranean Oligo-Miocene biostratigraphic evolution – the gastropods' point of view. *Paleogeography, Paleoclimatology, Paleoecology*, **183**, 103–133.

Hendler, G., Miller, J. E., Pawson, D. L. & Kier, P. M. 1995. Sea Stars, Sea Urchins and Allies – Echinoderms of Florida and the Carribbean. Smithonian Institute Press, Washington, London, 1–390.

Hessami, K., Koyi, H. A., Talbot, C. J., Tabasi, H. & Shabanian, E. 2001. Progressive unconformities within an evolving foreland fold-thrust belt, Zagros Mountains. *Journal of the Geological Society, London*, **158**, 969–981.

Hilgen, F. J., Krijgsman, W., Raffi, I., Turco, E. & Zachariasse, W. J. 2000. Integrated stratigraphy and astronomical calibration of the Serravallian/Tortonian boundary section at Monte Gibliscemi (Sicily, Italy). *Marine Micropaleontology*, **38**, 181–211.

Hilgen, F. J., Abdul Aziz, H., Krijgsman, W., Raffi, I. & Turco, E. 2003. Integrated stratigraphy and astronomical tuning of the Serravallian and lower Tortonian at Monte dei Corvi (Middle-Upper Miocene, northern Italy). *Paleogeography, Paleoclimatology, Paleoecology*, **199**, 229–264.

Hilgen, F. J., Abdul Aziz, H., Bice, D., Iaccarino, S., Krijgsman, W., Kuiper, K. F., Montanari, A., Raffi, I., Turco, E. & Zachariasse, W. J. 2005. The Global Boundary Stratotype Section and Point (GSSP) of the Tortonian Stage (Upper Miocene) at Monte dei Corvi. *Episodes*, **28**, 6–17.

Hsü, K. J., Ryan, W. B. F. & Cita, M. B. 1973. Late Miocene desiccation of the Mediterranean. *Nature*, **242**, 240–244.

Hubert-Ferrari, A., Armijo, R., King, G. C. P., Meyer, B. & Barka, A. 2002. Morphology, displacement and slip rates along the North Anatolian Fault

(Turkey). *Journal Geophysical Research*, **107**, 101029–101059.

Hüsing, S. K., Hilgen, F. J., Abdul Aziz, H. & Krijgsman, W. 2007. Completing the Neogene geological time scale between 8.5 and 12.5 Ma. *Earth and Planetary Science Letters*, **253**, 340–358.

Hubert-Ferrari, A., King, G., Van der Woerd, J., Villa, I., Altunel, E. & Armijo, R. 2009. Long-term evolution of the North Anatolian Fault. *In*: van Hinsbergen, D. J. J., Edwards, M. A. & Govers, R. (eds) *Collision and Collapse of the Africa–Arabia–Eurasia Subduction Zone*. Geological Society, London, Special Publications, **311**, 133–154.

IGRS-IFP, 1966. Étude Géologique de l'Épire (Grèce nord-occidentale). Paris, Institut Francais du Petrol.

Jacobs, E., Weissert, H. & Shields, G. 1996. The Monterey event in the Mediterranean: A record from shelf sediments of Malta. *Paleoceanography*, **11**, 717–728.

Jolivet, L. 2001. A comparison of geodetic and finite strain pattern in the Aegean, geodynamic implications. *Earth and Planetary Science Letters*, **187**, 95–104.

Jolivet, L. & Faccenna, C. 2000. Mediterranean extension and the Africa-Eurasia collision. *Tectonics*, **19**, 1094–1106.

Karig, D. E. & Kozlu, H. 1990. Late Paleogene–Neogene evolution of the triple junction region near Maraş, south-central Turkey. *Journal of the Geological Society, London*, **147**, 1023–1034.

Kaymakçi, N., Inceöz, M. & Ertepinar, P. 2006. 3D-Architecture and Neogene Evolution of the Malatya Basin: Inferences from the Kinematics of the Malatya and Ovacik Fault Zones. *Turkish Journal of Earth Sciences*, **15**, 123–154.

Keskin, M. 2003. Magma generation by slab steepening and breakoff beneath a subduction-accretion complex: An alternative model for collision-related volcanism in Eastern Anatolia, Turkey. *Geophysical Research Letters*, **30**, doi:10.1029/2003GL018019, 2003.

Krijgsman, W., Langereis, C. G., Daams, R. & van der Meulen, A. J. 1994. Magnetostratigraphic dating of the middle Miocene change in the continental deposits of the Aragonian type area in the Calayud-Terueal basin (Central Spain). *Earth and Planetary Science Letters*, **128**, 513–526.

Lamarck, J.-B. P. A. de M. 1804. Suite des mèmoires sur les fossiles des environs de Paris. *Annales de Museum Histoire Naturelle*, **5**, 179–357.

Le Pichon, X., Angelier, J. & Sibuet, J.-C. 1982. Plate boundaries and extensional tectonics. *Tectonophysics*, **81**, 239–256.

Linnaeus, C. 1758. *Systema naturae per regna tria naturae, secundum classes, ordines, genera, species, cum characteribus, differentiis, synonymis, locis. – Editio decima, reformata*. Holmiae.

Livermore, R., Nankivell, A., Eagles, G. & Morris, P. 2005. Paleogene opening of Drake Passage. *Earth and Planetary Science Letters*, **236**, 459–470.

Lourens, L. J., Hilgen, F. J., Shackleton, N. J., Laskar, J. & Wilson, D. 2004. The Neogene Period. *In*: Gradstein, F. M., Ogg, J. G. & Smith, A. G. (eds) *A geological time scale 2004*. Cambridge University Press, 409–440.

Mandic, O. 2000. *Oligocene to Early Miocene pectinid bivalves of Western Tethys (N-Greece, S-Turkey, Central Iran and NE-Egypt) – taxonomy and paleobiogeography*. Unpubl. PhD thesis, University of Vienna.

Mandic, O. & Piller, W. E. 2001. Pectinid coquinas and their paleoenvironmental implications – examples from the early Miocene of northeastern Egypt. *Paleogeography, Paleoclimatology, Paleoecology*, **172**, 171–191.

Martini, E. 1971. Standard Tertiary and Quaternary calcareous nannoplankton zonation. *In*: Farinacci, A. (ed.) Proceedings of the Second Planktonic Conference Roma, Edizioni Technoscienza, Roma. 739–785.

McClusky, S., Balassanian, S., Barka, A., Demir, A., Ergintav, S., Georgiev, I. *et al.* 2000. Global Positioning System constrains on plate kinematics and dynamics in the eastern Mediterranean and Caucasus. *Journal Geophysical Research*, **105**, 5695–5719.

Meulenkamp, J. E. & Sissingh, W. 2003. Tertiary paleogeography and tectonostratigraphic evolution of the Northern and Southern Peri-Tethys platforms and the intermediate domains of the African-Eurasian convergent plate boundary zone. *Paleogeography, Paleoclimatology, Paleoecology*, **196**, 209–228.

Miller, K. G., Wright, J. D. & Fairbanks, R. G. 1991. Unlocking the Ice House: Oligocene–Miocene oxygen isotopes, eustacy, and margin erosion. *Journal Geophysical Research*, **96**, 6829–6848.

Miller, K. G., Wright, J. D. & Browning, J. V. 2005. Visions of ice sheets in a greenhouse world. *Marine Geology*, **217**, 215–231.

Nyst, H. 1836. Recherches sur les coquilles fossiles de Kleyn–Spauwen et Housselt (Province du Limbourg). *Messager des Sciences et des Arts de la Belgique, ou Nouvelles Archives Historiques, Litteraires et Scientifiques*, **4**, 139–180.

Pearce, J. A., Bender, J. F., de Long, S. E., Kidd, W. S. F., Low, P. J., Guner, Y., Şaroğlu, F., Yilmaz, Y., Moorbath, S. & Mitchell, J. G. 1990. Genesis of collision volcanism in Eastern Anatolia, Turkey. *Journal of Volcanology and Geothermal Research*, **44**, 189–229.

Perinçek, D. 1979. *The geology of Hazro–Korudag–Cüngüs–Maden–Ergani–Hazar–Elazig–Malatya Area*. The Geological Society of Turkey.

Perinçek, D. & Cemen, I. 1990. The Structural relationship between the Eastern Anatolian and Dead Sea fault zones in southeastern Turkey. *Tectonophysics*, **172**, 331–340.

Perinçek, D. & Kozlu, H. 1983. Stratigraphy and structural relations of the units in the Afşin-Elbistan-Doğanşehir region (Eastern Taurus). *In*: Tekeli, O. & Göncüoğlu, M. C. (eds) Proceedings of the international symposium, Geology of Taurus Belt, MTA, Ankara, Turkey, 181–198.

Perinçek, D. & Õzkaya, I. 1981. Arabistan Levhasi Kuyzey Kenari Tektonik evrimi. Tectonic evolution of the northern margin of Arabian plate. *Yerbilimleri, Hacettepe Universitesi, Bulletin of Institute of Earth Sciences of Hacettepe University Beytepe Ankara*, **8**, 91–101.

Popov, S. V. 1993. Zoogeography of the Late Eocene Basins of Western Eurasia Based on Bivalve Mollusks. *Stratigraphy and Geological Correlation*, **2**, 103–118.

Reilinger, R., McClusky, S., Vernant, P., Lawrence, S., Ergintav, S., Cakmak, R. *et al.* 2006. GPS constraints on continental deformation in the Africa–Arabia–Eurasia continental collision zone and implications for the dynamics of plate interactions. *Journal of Geophysical Research*, **111**, V05411, doi:10.1029/2005JB004051.

Reuter, M., Piller, W. E., Harzhauser, M., Mandic, O., Berning, B., Rögel, F. *et al.* 2007. The Oligo-/Miocene Qom Formation (Iran): evidence for an early Burdigalian restriction of the Tethyan Seaway and closure of its Iranian gateways. *International Journal of Earth Sciences*, doi 10.1007/s00531-007-0269-9.

Richter, D., Mariolakos, I. & Risch, H. 1978. The main flysch stages of the Hellenides. *In*: Closs, H., Roeder, D. & Schmidt, K. (eds) *Alps, Apennines, Hellenides*. Inter-Union Commission on Geodynamics Scientific Report, **38**, 434–438.

Robertson, A. H. F. 2000. Mesozoic-Tertiary tectonic-sedimentary evolution of a south Tethyan oceanic basin and its margins in southern Turkey. *In*: Bozkurt, E., Winchester, J. A. & Piper, J. D. A. (eds) *Tectonics and Magmatism in Turkey and the Surrounding Area*. Geological Society, London, Special Publication, **173**, 97–138.

Robertson, A. H. F., Unlügenç, Ü. C., Inan, N. & Tasli, K. 2004. The Misis-Andirin Complex: a Mid-tertiary melange related to late-stage subduction of the Southern Neotethys in S Turkey. *Journal of Asian Earth Science*, **22**, 413–453.

Rögl, F. 1998. Paleogeographic considerations for Mediterranean and Paratethys Seaways (Oligocene to Miocene). *Annalen des Naturhistorischen Museums in Wien*, **99**, 279–310.

Rögl, F. 1999. Circum-Mediterranean Miocene Paleogeography. *In*: Rössner, G. & Heissig, K. (eds) *The Miocene Land Mammals of Europe*. Dr. Fritz Pfeil Verlag, München, 39–48.

Ruggieri, G. & Sprovieri, R. 1970. I microforaminiferi delle 'marne di S. Cipirello' Translated Title: Foraminifera of the San Cipirello marls. *Lavori Istituto Geologia Palermo*, **10**, 1.

Sancay, R. H., Bati, Z., Isik, U., Kirici, S. & Akca, N. 2006. Palynomorph, Foraminifera, and Calcareous Nannoplankton Biostratigraphy of Oligo-Miocene Sediments in the Muş Basin, Eastern Anatolia, Turkey. *Turkish Journal of Earth Sciences*, **15**, 259–319.

Şaroğlu, F. & Yilmaz, Y. 1986. Geological evolution and basin models during neotectonic episode in the Eastern Anatolia. *Bulletin Mineral Research and Exploration Institute of Turkey*, **107**, 61–83.

Schaffer, F. X. 1912. Das Miozän von Eggenburg. Die Fauna der ersten Mediterranstufe des Wiener Beckens und die geologischen Verhältnisse der Umgebung des Manhartsberges in Niederösterreich. Die Gastropoden der Miocänbildungen von Eggenburg. *Jahrbuch der k.k. geologischen Reichsanstalt*, **22**, 127–193.

Schauroth, F. Freiherr von, 1865. Verzeichnis der Versteinerungen in Herzoglichen Naturaliencabinett zu Coburg: mit Angabe der Synonyme und Beschreibung Vieler Neuer Arten, Sowie der Letzteren Abbildung auf 30 Tafeln. Coburg, Dietz'sche Hofbuchdruckerei.

Schlotheim, E. F. von. 1820. Die Petrefactenkunde auf ihrem jetzigen Standpunkte durch die Beschreibung seiner Sammlung versteinerter und fossiler Überreste des Thier-und Pflanzenreichs der Vorwelt erläutert. Gotha, Beckersche Buchhandlung.

Schneider, B. & Schmittner, A. 2006. Simulating the impact of the Panamanian seaway closure on ocean circulation, marine productivity and nutrient cycling. *Earth and Planetary Science Letters*, **246**, 367–380.

Şenel, M. 2002. *Geological Map of Turkey*, Ankara, MTA.

Şengör, A. M. C. & Yilmaz, Y. 1981. Tethyan evolution of Turkey: a plate tectonic approach. *Tectonophysics*, **75**, 181–241.

Şengör, A. M. C., Görür, N. & Şaroğlu, F. 1985. Strike-slip faulting and related basin formation in zones of tectonic escape: Turkey as a case study. *In*: Christie-Blick, N. (ed.) *Basin Formation and Sedimentation*. Society of Economic Paleontologists and Mineralogists Special Publications, **37**, 227–264.

Şengör, A. M. C., Özeren, S., Genç, T. & Zor, E. 2003. East Anatolian high plateau as a mantle-support, North–South shortened domal structure. *Geophysical Research Letters*, **30**, doi: 10.1029/2003GL017858.

Şengör, A. M. C., Tüysüz, O., Imren, C., Sakinc, M., Eyidogan, H., Görür, N., Le Pichon, X. & Rangin, C. 2005. The North Anatolian Fault: a new look. *Annual Reviews in Earth and Planetary Sciences*, **33**, 37–112.

Slack-Smith, S. M. 1998. Ostreoidea. *In*: Beesley, P. L., Ross, G. J. B. & Wells, A. (eds) *Mollusca: The southern synthesis*. Fauna of Australia, CSIRO Publishing, Melbourne, **5**, **Part A**, CSIRO Publishing, Melbourne, 268–274.

Spezzaferri, S. 1994. Planktonic foraminiferal biostratigraphy of the Oligocene and lower Miocene in the oceanic record. An overview. *Paleontographia Italica*, **81**, 1–187.

Spezzaferri, S. & Premoli Silva, I. 1991. Oligocene planktonic foraminiferal biostratigraphy and paleoclimatic interpretation from Hole 538A, DSDP Leg 77, Gulf of Mexico. *Paleogeography, Paleoclimatology, Paleoecology*, **83**, 217–263.

Telegdi-Roth, K. v. 1914. Eine oberoligozäne Fauna aus Ungarn. *Geologica Hungaria*, **1**, 1–77.

Turco, E., Hilgen, F. J., Lourens, L. J., Shackleton, N. J. & Zachariasse, W. J. 2001, Punctuated evolution of global climate cooling during the late Middle to early Late Miocene: High-resolution planktonic foraminiferal, oxygen isotope records from the Mediterranean. *Paleoceanography*, **16**, 405–423.

Tüysüz, N. & Erler, A. 1995. Geology and geotectonic implications of Kazikkaya area, Kagizman-Kars (Turkey). *In*: Örcen, S. (ed.) *Geology of the Black Sea Region*. Proceedings of the International symposium on the Geology of the Black sea Region, 7–11 September 1995, Ankara, Turkey. General directorate of mineral research and exploration and chamber of geological engineering, Ankara, 76–81.

van der Zwaan, G. J. & Gudjonsson, L. 1986. Middle Miocene–Pliocene stable isotope stratigraphy and paleoceanography of the Mediterranean. *Marine Micropaleontology*, **10**, 71–90.

van der Zwaan, G. J., Jorissen, F. J. & Stigter, H. C. 1990. The depth dependency of planktonic/benthic foraminiferal ratios: Constrains and applications. *Marine Geology*, **95**, 1–16.

van Hinsbergen, D. J. J., Hafkenscheid, E., Spakman, W., Meulenkamp, J. E. & Wortel, M. J. R. 2005*a*. Nappe stacking resulting from subduction of oceanic and continental lithosphere below Greece. *Geology*, **33**, 325–328.

van Hinsbergen, D. J. J., Kouwenhoven, T. J. & van der Zwaan, G. J. 2005*b*. Paleobathymetry in the backstripping procedure: Correction for oxygenation effects on depth estimates. *Paleogeography, Paleoclimatology, Paleoecology*, **221**, 245–265.

van Hinsbergen, D. J. J., Langereis, C. G. & Meulenkamp, J. E. 2005*c*. Revision of the timing, magnitude and distribution of Neogene rotations in the western Aegean region. *Tectonophysics*, **369**, 1–34.

van Hinsbergen, D. J. J., Zachariasse, W. J., Wortel, M. J. R. & Meulenkamp, J. E. 2005*d*. Underthrusting and exhumation: A comparison between the External Hellenides and the 'hot' Cycladic and 'cold' South Aegean core complexes (Greece). *Tectonics*, **24**, doi: 10.1029/2004TC001692.

Wade, B. S., Berggren, W. A. & Olsson, R. K. 2007. The biostratigraphy and paleobiology of Oligocene planktonic foraminifera from the equatorial Pacific Ocean (ODP Site 1218). *Marine Micropaleontology*, **62**, 167–179.

Westaway, R. 2003. Kinematics of the Middle East and eastern Mediterranean updated. *Turkish Journal of Earth Sciences*, **12**, 5–46.

Westaway, R. 2004. Kinematic consistency between the Dead Sea Fault Zone and the Neogene and Quaternary left-lateral faulting in SE Turkey. *Tectonophysics*, **391**, 203–237.

Woodruff, F. & Savin, S. M. 1989. Miocene deepwater oceanography. *Paleoceanography*, **4**, 87–140.

Woodruff, F. & Savin, S. M. 1991. Mid-Miocene isotope stratigraphy in the deep sea: high resolution correlations, paleoclimatic cycles, and sediment preservation. *Paleoceanography*, **6**, 755–806.

Wright, J. D., Miller, K. G. & Fairbanks, R. G. 1992. Early and Middle Miocene stable isotopes: implications for deepwater circulation and climate. *Paleoceanography*, **7**, 357–389.

Yilmaz, Y. 1993. New evidences and model on the evolution of the southeast Anatolian orogen. *Geological Society of America Bulletin*, **105**, 251–271.

Yilmaz, Y., Güner, Y. & Şaroğlu, F. 1998. Geology of the quaternary volcanic centers of east Anatolia. *Journal of volcanology and geothermal research*, **85**, 173–210.

Zachariasse, W. J. 1992. Neogene planktonic foraminifers from Sites 761 and 762 off Northwestern Australia. *Proceedings of the Ocean Drilling Program, Scientific Results*, **122**, 665–675.

Zachos, J., Pagani, M., Sloan, L., Thomas, E. & Billups, K. 2001. Trends, rhythms, and aberrations in global climate 65 Ma to present. *Science*, **292**, 686–693.